Title
Factors influencing juvenile Chinook Salmon growth in a modified floodplain landscape

Author
Holmes, Eric James

Publication Date
2022

Peer reviewed|Thesis/dissertation

Factors influencing juvenile Chinook Salmon growth in a modified floodplain landscape

By

ERIC HOLMES
THESIS

Submitted in partial satisfaction of the requirements for the degree of

MASTER OF SCIENCE

in

Ecology

in the

OFFICE OF GRADUATE STUDIES

of the

UNIVERSITY OF CALIFORNIA

DAVIS

Approved:

Robert A. Lusardi, Chair

Andrew L. Rypel

Peter B. Moyle

Committee in Charge

2022

Abstract:

Anthropogenically modified floodplains, such as flood bypasses, have increasingly received attention because of their potential to provide multiple societal functions including flood control, agriculture and ecosystem services. In many highly developed landscapes, these components of the contemporary riverscape represent remnants of historically vast seasonal floodplains. Characterizing the ecological role that these habitats play in the growth and life-history of Chinook Salmon, *Oncorhynchus tshawytscha*, is important for improving management of this imperiled species. Previous research indicates a high potential for off-channel floodplain habitats in these flood bypasses to support high lower trophic productivity and ideal growth conditions for juvenile Chinook Salmon. However, due to interannual variability in precipitation and dynamic hydrologic conditions inherent to the Mediterranean climate of California, the range and reproducibility of resulting habitat quality conditions requires additional growth experiments to inform conservation actions. To provide such context, we conducted 45 enclosure experiments, defined as a distinct location and year combination, spanning 4 habitat types: wetland, agriculture, river channel and canal channel within the Sutter Bypass and adjacent Sacramento River, Feather River, and Butte Creek. Experiments were conducted during wet (2019), dry (2020) and critically dry (2021) water years. During each enclosure experiment, we measured juvenile Chinook Salmon growth rates, water quality parameters (e.g. water temperature, dissolved oxygen, conductivity, pH, and chlorophyll-α), zooplankton density, and salmon diets. This high spatiotemporal replication and trophic level coverage allowed characterization of habitat quality for juvenile Chinook Salmon under a wide range of environmental conditions. During experiments, we also sampled wild juvenile Chinook Salmon to assess habitat usage of the Sutter Bypass and Butte Sink. Across all years, we found distinct water quality conditions and zooplankton communities associated with off-channel habitats. Wetland habitats supported the fastest salmon growth rates in all years (range 0.36-0.98 $mm \cdot day^{-1}$), but magnitude of difference was less in the wet year. River channel habitats displayed the lowest heterogeneity in salmon growth response both spatially and temporally (range 0.15-0.37 $mm \cdot day^{-1}$), while agriculture and canal channel habitats of the Sutter Bypass displayed higher heterogeneity in salmon growth (range 0.31-0.68 and 0.08-0.89 $mm \cdot day^{-1}$ respectively). A boosted regression tree model with abiotic and biotic factors indicated the importance of key prey items and primary production for salmon growth response. Findings suggest that the growth potential of juvenile salmon is 1) variable through time and dependent on hydrologic conditions and 2) variable through space and strongly dependent on prey availability in various habitat types.

Dedication:

This thesis is dedicated to the wonderful family, friends, and colleagues who supported me selflessly throughout. Carson, thank you for being a great mentor and patient friend throughout this adventure. Flora, your tireless work ethic inspires me to never let anything come between me and my goals, vive la spring run! Matt, your curiosity and excitement for everything that moves, or doesn't anymore, is infectious and it's been a pleasure catching fish and bugs with you. Rob, I appreciate your guidance and how you welcomed me into your lab with support and open arms. Peter and Andrew, you inspire me to work tirelessly to conserve the amazing freshwater ecosystems of California and beyond. Rachel, I appreciate your confidence in me and I aspire to be a scientist and person even a fraction of your caliber. Cathryn, thank you for the support you have provided to me and my fellow researchers. To my colleagues Miranda, Mollie, Ryan, Sarah, Ann, Malte, Nick, Lily, Gabe, and the rest of the Watershed Center family, you made our building a warm and wonderful place for learning and accomplishing great things. I could never have done this without the unwavering support of my better half, Katelin, you mean the world to me. To Hunter, the math-magician, you inspire me to never shy away from an equation. To Elise, the creative mastermind, you inspire me to innovate and never give up. To Anne and Steve, I wouldn't be here without you.

Introduction:

Habitat loss and land use conversion have been implicated as leading causes of species decline worldwide (Foley et al., 2005), and have disproportionately affected freshwater ecosystems (Strayer and Dudgeon, 2010; Geist, 2011). Among freshwater habitats, floodplains are one of the most degraded habitats with numerous consequences for freshwater biodiversity documented across the world (Tockner and Stanford 2002; Nilsson et al. 2005; Knox et al. 2022;). Loss of floodplain habitat, in particular, has strongly impacted endemic and native fishes (Aarts et al. 2004; Welcomme, 2008; Arthington and Balcombe, 2011). Consequently, multifunctional floodplain management has been recently proposed as a key concept to improve declining biodiversity and ecosystem services (Schindler et al. 2016), particularly in California's Central Valley (CCV). Few studies have looked at how salmon populations use and benefit from the current state of anthropogenically modified floodplains, such as flood bypasses. Initial work suggests that floodplain processes which support ecosystem services are compatible with flood control and farming (Sommer et al., 2001b; Jeffres et al., 2020; Holmes et al 2021; Cordoleani et al. 2022). This highlights the potential for a reconciliation approach where ecological needs are accounted for in the midst of human-dominated landscapes (Rosenzweig, 2003).

Severe habitat alterations of the landscape have led to dramatic declines of Chinook Salmon populations in the CCV (Yoshiyama, 1998, Katz et al., 2013). The CCV historically provided juvenile Chinook Salmon with a productive rearing environment composed of a complex mosaic of riparian habitat with meandering river channels and approximately 1.6 million ha of ephemeral wetland habitat (Fretwell, 1996). Today, the highly altered landscape of the CCV, with its extensive flood control system of dams and levees, has reduced historical floodplain habitat by approximately 93% (Herbold et al., 2018). Remnant floodplain habitat exists in a series of multi-use flood bypasses which provide flood protection to nearby cities. Sommer et al. (2001a) found that some of these habitats (i.e. the Yolo Bypass) can function as high quality habitat for juvenile salmon with specific fitness benefits to growth

and survival. However, due to the dynamic nature of these systems, this work and others (Jeffres et al., 2008; Katz et al., 2017; Holmes et al. 2021; Cordoleani et al., 2022) suggest a need to better understand spatiotemporal heterogeneity in habitat quality, including effects on Chinook Salmon growth.

The difficulty of characterizing spatiotemporal variability in habitat quality for juvenile salmon stems from uncertainty in habitat usage and variability in response to dynamic hydrologic conditions (Sommer et al., 2020). Additional challenges are associated with periodic hydrologic shifts connecting flood bypass habitats to rivers and subsequent changes in floodplain water residence time and connectivity. Previous work on zooplankton (important prey for juvenile salmon) community structuring suggests certain zooplankton species (e.g. *Daphnia Spp., Calanoid Spp.*) are indicative of long-residence times of water (Corline et al., 2021) and have the potential to support high salmon growth when present. This continuum of hydrologic connectivity in the river-floodplain corridor results in highly variable abiotic and food availability conditions with relatively little understanding of how these changes might affect juvenile salmon growth. To resolve these questions, we designed a series juvenile Chinook Salmon enclosure experiments spanning the primary habitat types present in the northern CCV landscape.

We investigated landscape-scale hydrologic, water quality, and lower trophic metrics in representative habitats from experiments conducted over a three-year period to understand how biotic and abiotic environmental characteristics correlate with variation in enclosure-reared salmon growth. Habitats included main-stem river channel, bypass canal channel, off-channel agricultural and off-channel wetland sites. Concurrent wild salmon sampling of body size, habitat occupancy, and diets are compared with results from an enclosure experiment to provide context for inferred relative habitat benefits to wild salmon populations in the Sacramento River, Feather River, and Butte Creek watersheds. We hypothesized that water year type and associated hydrologic conditions would affect

physical water quality parameters, primary production metrics, and lower trophic communities across habitat types leading to differential growth rates of juvenile Chinook Salmon across study years.

Methods:

Study area

California's Mediterranean climate has distinct dry and wet seasons and highly variable annual precipitation totals which are often determined by the latitude of a few land-falling atmospheric river events originating in the Pacific Ocean (Dettinger et al., 2011). Snowmelt and rainfall runoff in the Northern Sierra Nevada and Southern Cascade Mountains feeds the Sacramento River watershed which run through the highly developed Sacramento Valley en route to the ocean. The Sutter Bypass is the northernmost most flood bypass in the Sacramento Valley, encompassing approximately 14,000 ha from the Butte Sink in the north to the confluence with the Feather and Sacramento Rivers at Verona in the south (see Figure 1). In late winter and spring, Sacramento River water can flow into the Butte Sink via Moulton weir and the Sutter Bypass via Colusa, and Tisdale weirs. The Butte Creek watershed connects to the Butte Basin just north of the Sutter Buttes. The low lying topography of the Butte Sink and Sutter Basin combined with the design of the weir infrastructure at the Sacramento River results in the Sutter Bypass flooding nearly every year. This crucial piece of the Central Valley Project relieves stage pressure on the levees of the Sacramento and Feather Rivers. The periodic inundation of the Bypass allows some natural flood processes to persist in an altered hydrologic landscape. These processes provide ecosystem services such as groundwater recharge, food web production, and off-channel habitat for aquatic species (Sommer et al. 2001b; Grosholz and Gallo 2006; Opperman et al. 2009).

The Butte basin in the lower portion of the Butte Creek watershed retains a large area of interconnected wetlands and sloughs managed primarily for waterfowl habitat and hunting. Riparian water rights and irrigation infrastructure ensures that this area is inundated every year for a prolonged period during winter and spring (Garone, 2020). The low lying-topography and frequent inundation from

the unregulated Butte Creek and from overflow of the Sacramento River, make this area generally unsuitable for agriculture and development. The managed river-wetland corridor that remains is suitable for waterfowl habitat and hunting purposes. Wetland effluent from the lower Butte Sink area coalesces back into a single slough channel, Butte Slough. Water can be then either be directed through the one-way Butte Slough Outfall Gate (BSOG) into the Sacramento River downstream of Colusa or diverted south through the Sutter Bypass borrow canal channels. These Bypass canal channels are used for water distribution and drainage for agriculture and managed wetlands. The canal channels coalesce with the Sacramento River at the terminus of the Sutter Bypass via Sacramento Slough which is located immediately upstream of the Feather River Confluence.

Sampling locations

Over a three-year period, 19 locations were selected for the juvenile Chinook Salmon enclosure experiment across five regions of interest: 1) Butte Sink: North of Colusa weir, 2) Upper Bypass: Colusa weir to Tisdale weir, 3) Lower Bypass: Tisdale weir south to Sacramento River, 4) Sacramento River, and 5) Feather River (Table 1, Figure 1). Four different habitat types were investigated: main-stem river channel, bypass canal channel, off-channel agricultural and off-channel wetland (Table 1). River channel and wetland sites from 2019 were replicated in 2020 and 2021, with the exception of SRC1 which was moved downstream approximately 1km in 2020 and 2021. Based on observations from 2019 experiment, canal channel sites were added in the Butte Sink and Sutter Bypass in 2020 and 2021, with the expectation of moving the enclosures from the canals to adjacent off-channel sites during flooding. However, flooding did not occur during those years, so initial canal channel sites were used during the entire experiment. Due to lack of flooding in 2020, no off-channel agriculture habitat sites were available. Similarly, in 2021 no natural flooding of agricultural sites occurred, but one agriculture site (BSA1) was intentionally flooded using irrigation infrastructure.

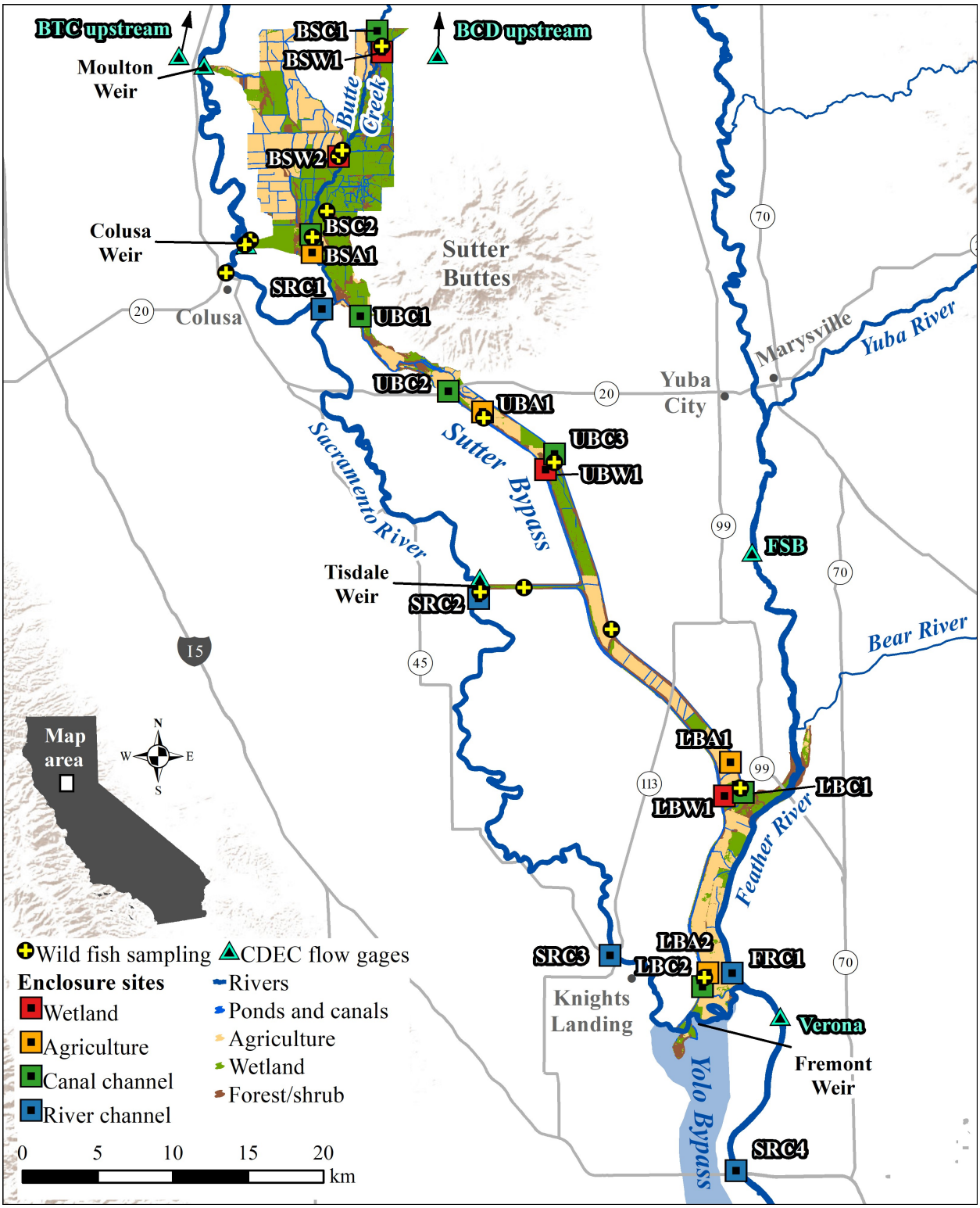

Figure 1: *Map of water bodies adjacent to the Sutter Bypass. Sutter Bypass is shown with land use coverage from the National Land Cover Database, the USDA Cropland Data Layer, and the National Water Information System. Point data includes enclosure locations (squares), wild fish sampling sites (circles with crosses), and flow gages (triangles).*

Table 1: *Table of enclosure sites with the region, site name, habitat type, latitude, longitude, and years where samples were collected at each location.*

Region	Site	Habitat type	Latitude	Longitude	Years
Butte Sink	BSW1	Wetland	39.3481	-121.890	2019, 2020, 2021
	BSW2	Wetland	39.2858	-121.925	2019, 2020, 2021
	BSC1	Canal channel	39.3607	-121.894	2019, 2020, 2021
	BSA1	Agriculture	39.2350	-121.947	2021
	BSC2	Canal channel	39.2398	-121.948	2021
Upper Bypass	UBC1	Canal channel	39.1900	-121.909	2020, 2021
	UBC2	Canal channel	39.1445	-121.842	2020, 2021
	UBA1	Agriculture	39.1277	-121.815	2019
	UBW1	Wetland	39.0988	-121.761	2019, 2020, 2021
	UBC3	Canal channel	39.1027	-121.759	2020, 2021
Lower Bypass	LBA1	Agriculture	38.9180	-121.627	2019
	LBW1	Wetland	38.9026	-121.624	2019, 2020, 2021
	LBC1	Canal channel	38.9018	-121.620	2020, 2021
	LBA2	Agriculture	38.7916	-121.651	2019
	LBC2	Canal channel	38.7859	-121.653	2020, 2021
Sacramento River	SRC1	River channel	39.2094	-121.988	2019, 2020, 2021
	SRC1	River channel	39.1946	-121.939	2019, 2020, 2021
	SRC2	River channel	39.0202	-121.821	2019, 2020, 2021
	SRC3	River channel	38.8054	-121.724	2019, 2020, 2021
	SRC4	River channel	38.6754	-121.630	2019, 2020, 2021
Feather River	FRC1	River channel	38.7936	-121.631	2019, 2020, 2021

Hydrology

Hydrologic data were obtained from the California Data Exchange Center (CDEC, cdec.water.ca.gov) for the Sacramento River at Butte City (CDEC station ID: BTC), Feather River at Boyd's landing (CDEC station ID: FSB), and Butte Creek at Durham (CDEC station ID: BCD). Weir overtopping data for the three Sutter Bypass weirs, Moulton, Colusa, and Tisdale, were also obtained through CDEC (CDEC station IDs: MLW, CLW, TLW, respectively). Historical daily hydrologic data were obtained from the USGS for the Sacramento River at Bend Bridge (USGS Station ID: 11377100) for the period 1893 to 2021 which spanned natural hydrologic and regulated hydrologic conditions after the construction of the Shasta dam completed in 1943. Median discharge and 90th quantile flows were computed for the periods before and after Shasta Dam completion and displayed in an annual hydrograph format. Mean

December through April discharge was calculated and displayed on frequency histograms faceted by pre and post dam completion. A flooding threshold of 566.3 cms was set for the Sacramento River at Bend Bridge based on an approximate flooding threshold of 651.3 cms at the Tisdale weir crest while accounting for some accretion flows of two tributaries, Thomes Creek and Stony Creek, downstream of Bend Bridge. Days above the threshold were tallied by year and displayed in a probability density plot with overlaid density curve separated by pre- and post-Shasta dam completion. Empirical cumulative distribution functions for annual flooded days were displayed on the same x-axis as the probability distribution function to highlight differences in the hydrology pre- and post-Shasta dam completion.

Water quality

Water quality sampling was performed weekly at all enclosure locations from 1/7 to 4/29 in 2019, from 1/13 to 3/18 in 2020 and from 1/25 to 3/29 in 2021. Point water quality data was collected weekly at all locations with an Exo2 multiparameter sonde (YSI, Yellow Springs, OH). The parameters collected included: temperature (°C), dissolved oxygen percent saturation (%), dissolved oxygen concentration ($mg \cdot L^{-1}$), turbidity (NTU), chlorophyll-α concentration ($\mu g \cdot L^{-1}$), relative blue-green algae concentration ($\mu g \cdot L^{-1}$), electrical conductivity ($\mu S \cdot cm^{-1}$), total dissolved solids (, salinity (PSU), and pH. In 2020, due to sonde malfunction and overlapping project use on a few occasions, sonde measurements were not taken in some weeks.

Water grab samples were used for laboratory water chemistry analysis at the University of California, Davis. The parameters analyzed included dissolved organic carbon (DOC; ppm), chlorophyll-α (ppb), and pheophytin α (ppb). In 2020, due to the global COVID19 pandemic, the lab responsible for processing water samples was closed and our samples from the majority of the project expired and were disposed of without being analyzed.

Continuous water temperature (°C) was collected at all enclosure sites with either U22 or U26 loggers (Onset Corporation, Bourne, MA) during juvenile salmon growth studies. Dissolved oxygen

($mg \cdot L^{-1}$) was collected at a subset of sites (n = 6) in 2019 and at all cage locations in 2020 and 2021 using U26 loggers continuously recording at a 15-minute interval and suspended approximately 0.5 meters below the water surface.

Zooplankton sampling

Zooplankton sampling occurred weekly, at all enclosure locations. Samples were collected using a 15 cm or 30 cm diameter 150 µm mesh zooplankton net thrown five meters and retrieved through the water column four times from the stream bank. To account for differences in sampled volume due to variable water velocities, a flow meter attached to the zooplankton net was used to quantify the volume of water sampled. All samples were preserved in a solution of 95% ethanol and were processed for invertebrate species identification at the UC Davis Center for Watershed Sciences lab. Invertebrate densities ($individuals \cdot m^{-3}$) were estimated for all enclosure locations.

Invertebrate subsampling was necessary due to the high density of invertebrates within samples. Samples were rinsed through a 150 µm mesh and emptied into a beaker. The beaker was filled to a known volume to dilute the sample, depending on the density of individuals within the sample, and sub-sampled with a 1mL large bore pipette. If densities were still too great for enumeration, the sample was split using a Folsom splitter before sub-sampling with the bore pipette. The dilution volume, number of splits, and number of aliquots removed was recorded and used to obtain total estimates of invertebrates which were divided by the total volume sampled to estimate density. Invertebrate samples were sorted into two groups of one hundred. One group was for the taxonomic group with the highest amount of individuals counted. A second group was for the total individual counts of each of other taxonomic groups added up such that they met or exceeded a hundred in total numerical count. If a hundred of the single highest taxonomic group was reached, but not a hundred of the remaining total individuals, then in the following aliquots the highest taxonomic group was not counted. Invertebrates were identified with the aid of a dissecting microscope at 4x magnification to the lowest taxonomic level

possible using various taxonomic keys from Merritt and Cummins (1996), Thorp and Covich (2009), and Karanovic (2012).

Zooplankton taxa were grouped into higher taxonomic units (HTUs) for plotting and analysis components. The HTUs were comprised of large-bodied Cladocera, small-bodied Cladocera, Copepoda, Ostracoda, Rotifera, and Insecta categories. Cladoceran species were broken into two groups based on body size (threshold = 1mm, Dumont et al., 1975) based on Brooks and Dodson (1965) who showed how fish predation controlled species composition. Similar patterns may be present in perennial and ephemeral habitats that we sampled based on relative predation pressure.

Salmon enclosure experiment

We used an enclosure study design where individually marked fish were kept in a fixed location in a small enclosure during a 4-6-week period. Similar enclosure experiments have been used in past studies to identify differences in habitat suitability (Aha et al., 2020; Jeffres et al., 2008). We assessed a specific location through time and how fish growth responded to variable environmental conditions. Enclosures provide a controlled view of a specific location at the cost of behavioral modification (e.g. fish cannot search for more food rich areas, move to cooler waters at inlets, etc.).

Juvenile young-of-the-year fall-run Chinook Salmon were obtained from the Feather River State Hatchery in 2019, and Coleman National Fish Hatchery in 2020 and 2021. Each enclosure site had two 61cmx61cmx122cm floating cages constructed with 2.54cm (1-inch schedule 40) pvc pipe frames enclosed with 0.6cm plastic mesh material, allowing prey items to enter the cages. Each cage was stocked with 5 individually PIT tagged juvenile salmon which was based on densities from past enclosure experiments (Jeffres et al., 2020; Aha et al., 2021). Density within cages was maintained throughout the experiment by adding “placebo” hatchery fish when escape or mortality occurred among the marked fish. The caged salmon were measured for fork length (FL) to the nearest millimeter and weighed wet to the nearest 1/100th of a gram (g) with an Ohaus Scout Pro scale, at a two-week interval. Mass specific

growth rates ($SGR_i = 100 \times ln(end\_mass_i) - ln(start\_mass_i) / t$) were also calculated for each enclosure fish (i) at each two-week interval (where t = days between sampling events), to remove the influence of body size on absolute growth for interim growth measurements with variable fish starting size. We excluded data from UBC3 in 2021 due to vandalism of our enclosures resulting in fish loss after the second week. Similarly, enclosure data was unavailable for LBC1 in 2021 due to channel dewatering as a result of the critical drought conditions.

Enclosure salmon diet

Salmon diets were obtained from euthanized fish from the growth experiment at the end of the experiment and from fish sampled from an additional "diet" enclosure which was sampled at a 1-week interval at one enclosure site per region in 2019 and at all enclosure locations at a 2-week interval in 2020 and 2021. Stomach contents from the euthanized enclosure salmon were identified to their lowest practical taxonomic group with the aid of a dissecting microscope. Due to the partial digestion of the prey items, the identification was generally limited to the order taxonomic level for analysis. Total prey wet weight in g was measured by the difference between the full stomach weight and the reweighed stomach with the contents removed. Prey mass index (PMI) was calculated with the following formula: PMI *= 100 * prey wt/(fish wt – prey wt).* This index allowed comparison of prey weights between different sized salmon.

Wild salmon sampling

Wild fish sampling was conducted to determine wild fish occupancy, size distribution, and diet composition in a variety of habitats and hydrologic conditions. Wild fish were sampled using 9m wide and 5mm mesh beach seines or fyke net traps. Wild fish sampling events were opportunistic and targeted juvenile Chinook Salmon.

Captured salmon were measured to the nearest millimeter and weighed to the nearest 1/100th of a gram. Additionally, genetic fin clips were removed from one of the caudal lobes and standardized

photographs were taken for all juvenile salmon using methodology from Holmes and Jeffres (2021). A subsample of 120 fall-run size juvenile Chinook Salmon were euthanized and analyzed for diet contents using the same methods as for enclosure-reared salmon. Other fish species caught during these sampling efforts were enumerated and up to the first 30 from a given sampling location/date were measured for fork length (mm) where applicable and total length when no caudal fin fork existed (e.g. lamprey).

Statistical analyses

Non-parametric ANOVA

Rank-based comparison of water quality and zooplankton samples from different habitats and years was conducted with a Kruskall-Wallis test and a post-hoc Dunn test for pairwise comparison of means. Non-parametric ANOVA equivalents were selected due to violations of the assumption of normality. A Bonferroni correction was applied to the alpha threshold to account for the increased potential of a Type-I error due to the sheer number of hypothesis tests conducted. The results from the pairwise comparison of means were displayed with compact letter displays (CLD) in the boxplot facets associated with the unique parameter/year/habitat combinations to show significance groups. The significance threshold was set at an $\alpha = 0.05$ level.

Non-metric multidimensional scaling analysis

Zooplankton community analysis and enclosure-reared salmon stomach content analysis was performed on the HTU densities and counts respectively using a non-metric multidimensional scaling (NMDS) approach. We used bi-weekly zooplankton HTU total densities (organisms$\cdot m^{-3}$), to correspond with the growth measurement periods. Bi-weekly densities were Hellinger transformed prior to community analysis due to the reduced sensitivity to rare species (Legendre and Gallagher, 2001). A global NMDS analysis including data from all three years with output plotted for individual years separately to visually show interannual variability on consistent axes. NMDS analyses (figures presented

in supplemental information) and associated analysis of similarity (ANOSIM) tests were conducted on data from individual years to test for differences in zooplankton community assemblages and enclosure salmon diets between habitat types for each year. All NMDS analyses had two dimensions and stress scores are presented in the results section.

Growth rate response model

A boosted regression tree (BRT) approach was employed using the *dismo* R package with mass specific growth rate as the response variable to identify the environmental factors correlated with growth rates following methodology presented in Elith et al. (2008). The BRT approach was chosen due its ability to identify non-linear responses, such as thresholds, to explanatory variables. Additionally, BRT models are conducive for high dimensional data, predictor variable interactions, and collinearity (Elith et al., 2008). Biotic and abiotic explanatory variables were aggregated for each approximate 2-week period between fish sampling events. Exceptions to the 2-week aggregation interval included: 1) in 2019 when BSW2 was inaccessible due to widespread flooding in week 2 and sampling was delayed until week 3, and 2) an early termination of the experiment in 2020 at week 5 due to the global COVID19 pandemic led to all final period lengths to be 1 week.

Software

All analyses were conducted in R version 4.2 (R Core Team, 2022). NMDS and ANOSIM analyses were conducted with the *vegan* package (Oksanen et al., 2013). The boosted regression tree analysis was conducted with the *dismo* R package (Hijmans et al., 2021). All plotting was done with *ggplot2* R package (Wickham et al., 2016).

Results:

Hydrology

The regulation of river flows in large upstream reservoirs results in an altered runoff regime (Figure 2A) which has a multimodal distribution of seasonal average flow (Figure 2B). This is exemplified

in mean Dec-Apr runoff which shows three distinct modes of low runoff (<400 cms), moderate runoff (400-700 cms), and high runoff (> 700 cms). Low runoff years are the most common after Shasta dam completion (45% of years). The range of days exceeding the Sutter Bypass flood threshold before and after Shasta dam completion remains similar, however the probability density function has shifted towards less days of flooding annually post dam construction (Figure 2C and D). Historically, years with zero qualifying flood events, classified as over 566.3 cms for two or more days, exhibited a recurrence interval of 30.5 years (3.2% occurrence probability) before Shasta dam completion compared to a recurrence interval of 5.2 years (19.2% occurrence probability) post-dam construction (Figure 2D).

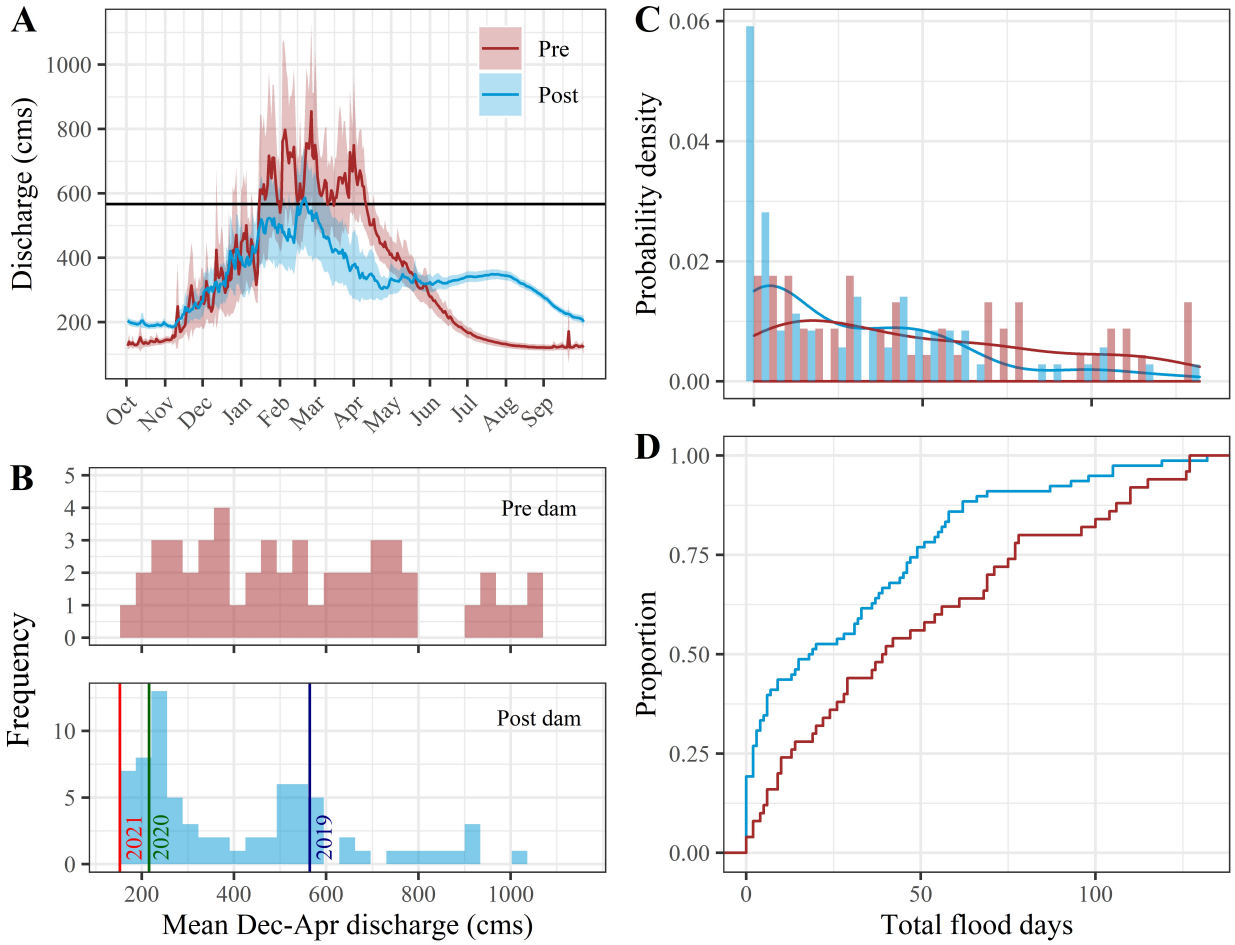

Figure 2. Panel A*: Hydrographs showing the median annual discharge in the Sacramento River at Bend Bridge from before (red) and after (blue) Shasta Dam completion in 1943 with shaded regions representing 90 percent confidence bands and an approximated horizontal activation threshold of 566 cms in black.* ***Panel B****: Histograms of mean December through April discharge with pre-dam (red, top)*

and post-dam (blue, bottom) completion and vertical lines to show 2019-2021 values. ***Panel C****: Probability density function for days exceeding a flood threshold colored by red and blue respectively.* ***Panel D****: An empirical cumulative density function (ecdf) for the Sacramento River at Bend Bridge with pre- and post-dam completion colored by red and blue respectively.*

Water years 2019-2021 exhibited variable precipitation with 2019 classified as a wet year, 2020 as a dry year, and 2021 as critically dry by the California Department of Water Resources (https://cdec.water.ca.gov/reportapp/javareports?name=WSIHIST). Despite precipitation extremes, the water years 2019 and 2020 fell roughly in the center of the moderate runoff and low runoff modes respectively, and therefore were a good representation of contemporary water year runoff types (Figure 2B). Water year 2021 provides insight into how the system functions during extremely dry conditions since this year exhibited the lowest Dec-Apr runoff on record due it being the second driest Northern California precipitation year compounded by low reservoir storage from the severe drought the previous year.

Flows in the Sacramento and Feather Rivers are regulated by California's two largest reservoirs, Lake Shasta and Lake Oroville respectively, and are managed with similar hydrologic regimes. During water year 2019 the hydrographs included multiple tributary-dominated flood events in January and February, followed by additional flood events which were heightened by increased and sustained reservoir releases from Shasta and Oroville dams. Butte Creek has small diversion dams, but as an unregulated tributary also exhibited numerous large flow pulses during 2019. This resulted in multiple overbank flows and substantial floodplain inundation in the Butte Sink, but less sustained overbank flows later in the season compared to the larger regulated rivers (Figure 3).

During 2020, there were a few early season tributary flow pulses, one of which approached the Tisdale weir threshold, but none registered on the weir stage gauge as an overtopping event. These minor flow events preceded an extended mid-season dry period with only minor flow pulses at the end of March and early April. 2021 was critically dry and like 2020 exhibited zero weir overtopping events. There were more precipitation events in 2021; however, these weather systems were moisture-

deficient yielding small amounts of precipitation and relatively cold with lower snow line elevations which resulted in reduced river runoff.

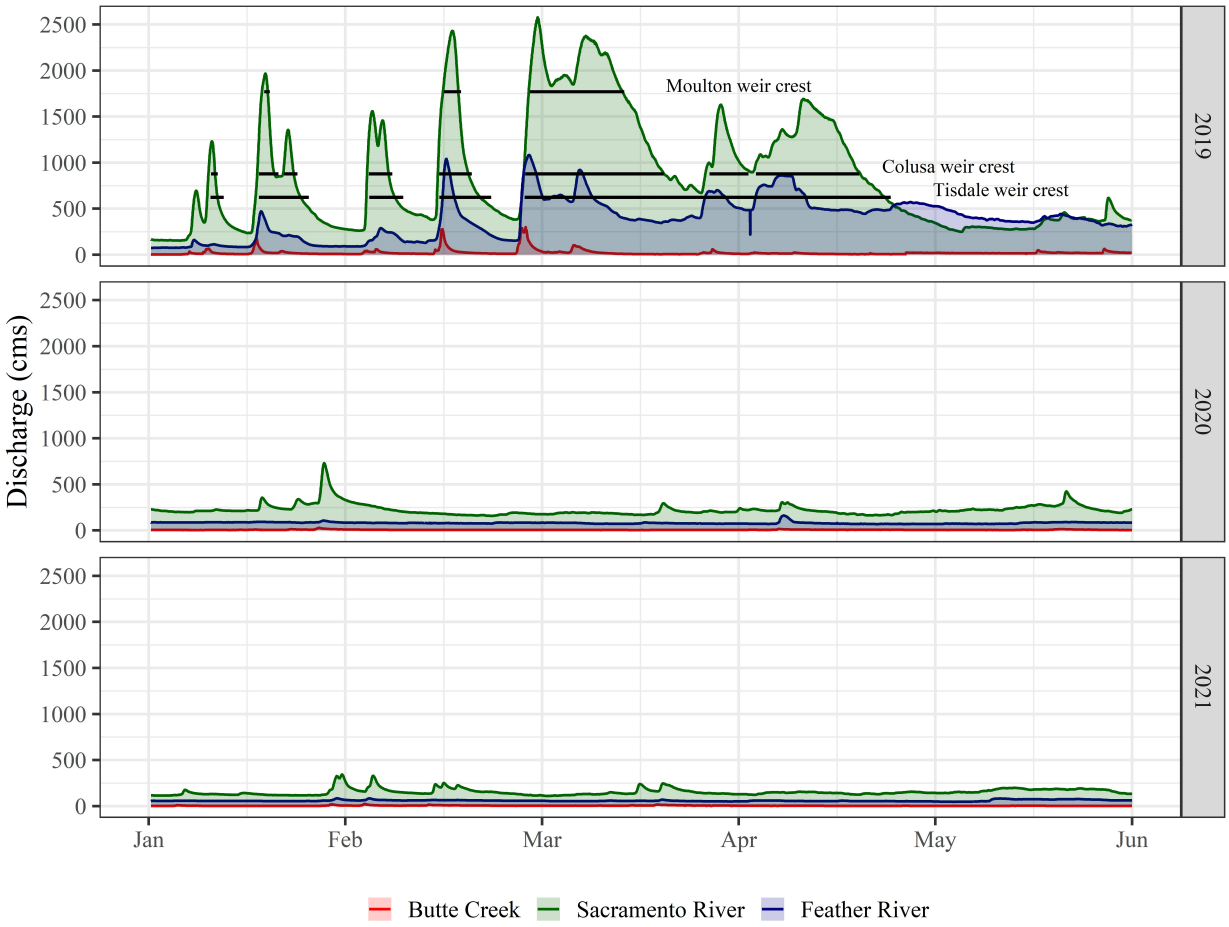

Figure 3. Hydrographs for 2019 to 2021 for the three primary tributaries of the Sutter Bypass, including the Sacramento River (green), Feather River (blue), and Butte Creek (red). Observed weir overtopping events for Moulton, Colusa, and Tisdale weirs are displayed by the black horizontal lines set at the approximate weir overtopping discharge thresholds.

Water quality

Water temperatures in river and canal channel habitats were generally more stable and cooler in all years compared to off-channel habitats (Figure 4A). Conversely, off-channel habitats exhibiting shallower depths, large aerial extents, and low to periodically zero flowing water showed water temperature profiles which were more closely related to atmospheric conditions with high diurnal fluctuations (see “rangetemp” in Figure 5). The exception to this pattern occurred during periods of

flooding of off-channel habitats where increased depth and high flows resulted in a river-dominated pattern with cooler mean temperatures and reduced diurnal variation. Despite higher daily maximum temperatures experienced in the off-channel habitats, the means were similar between channel and off-channel habitats due to the nightly decrease in temperature (Table 2).

Table 2. *Mean water temperature with standard deviation (°C) and range of water temperature (°C) observed at each enclosure site and year combination.*

Habitat	Site	Mean temperature ± SD (°C)			Temperature range (°C)		
		2019	2020	2021	2019	2020	2021
Wetland	BSW1	13.1 ± 2.8	13.4 ± 1.8	12.5 ± 1.3	7.1 to 19.6	8.8 to 18.2	9.7 to 16.5
	BSW2	13.4 ± 2.9	13.6 ± 2.4	12.3 ± 2.0	6.4 to 19.9	6.5 to 21.2	6.5 to 17.5
	LBW1	12.9 ± 2.5	14.5 ± 2.6	12.6 ± 2.2	7.1 to 19.8	7.5 to 22.2	5.8 to 20.2
	UBW1	13.0 ± 2.7	13.7 ± 2.9	13.5 ± 3.2	6.8 to 21.7	7.2 to 22.9	6.1 to 22.9
Agriculture	BSA1			12.8 ± 3.4			4.9 to 21.8
	LBA1	13.1 ± 2.3			7.4 to 19.6		
	LBA2	12.4 ± 1.7			10.1 to 17.2		
	UBA1	12.3 ± 2.3			8.4 to 17.5		
Canal channel	BSC1	11.1 ± 1.4	12.8 ± 1.3	11.7 ± 1	7.6 to 13.8	9.4 to 16	9.7 to 14.5
	BSC2			12.6 ± 0.9			10.4 to 15.0
	LBC1		14.2 ± 0.7			11.1 to 15.5	
	LBC2		13.6 ± 1.7	12.2 ± 1.9		9.8 to 19.2	4.3 to 22.4
	UBC1		14.5 ± 1.8	12.8 ± 1.0		9.9 to 18.5	10.8 to 16.4
	UBC2		14.1 ± 1.5	12.7 ± 0.9		7.8 to 21.5	10.6 to 15.1
	UBC3		14.0 ± 1.3	12.7 ± 0.7		10.7 to 17	11.3 to 15.9
River channel	FRC1	10.3 ± 0.9	13.1 ± 1.4	12.4 ± 0.9	8.2 to 12.1	10.1 to 16.6	10.1 to 14.9
	SRC1	10.6 ± 1.2	12.5 ± 0.9	11.6 ± 0.9	8.1 to 13.3	10.5 to 15.1	9.9 to 14.1
	SRC2	10.5 ± 1.2	12.6 ± 1.0	11.8 ± 0.8	6.9 to 13.0	10.1 to 15.1	10 to 13.8
	SRC3	10.6 ± 1.2	12.7 ± 1.0	11.8 ± 0.7	6.4 to 13.1	9.7 to 15.1	10.3 to 13.5
	SRC4	11.1 ± 1.3	12.8 ± 1.2	12.1 ± 0.8	8.4 to 14.2	9.7 to 15.3	10.5 to 14.2

Dissolved oxygen patterns were similar to the water temperature patterns in that the channel habitats exhibited stable dissolved oxygen levels which remained near saturation (Figure 4B). Conversely, off-channel habitats showed dissolved oxygen levels which displayed high diurnal variation. Similar to water temperature patterns, the dissolved oxygen diurnal range in off-channel habitats was muted during flood events. The periods of super-saturation of dissolved oxygen, generally above 10 $mg_{*}L^{-1}$ depending on water temperatures, in the wetlands indicated periods of high algal primary

production (Figure 4B). Periods where dissolved oxygen levels approached zero indicated high respiration rates by a combination of microbes, zooplankton, photosynthetic algae and plants, and fish. These low oxygen conditions generally coincided with periods of low to zero inflow, cloud coverage which limited photosynthetic oxygen production, and low wind which reduced mechanical aeration.

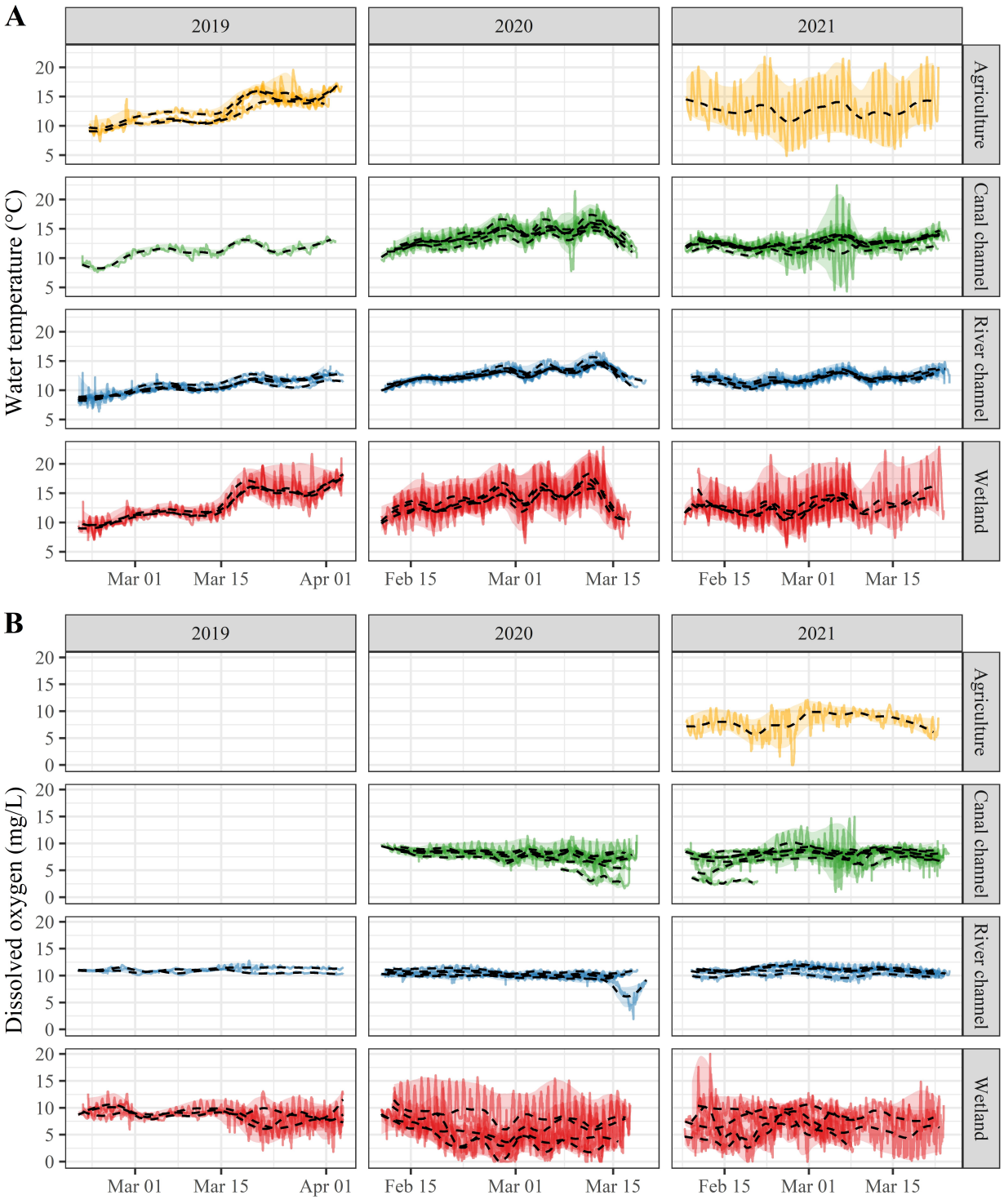

Figure 4. ***Panel A****: Continuous water temperature (°C) collected at 15-minute intervals.* ***Panel B****: Continuous dissolved oxygen collected at 15-minute intervals. Measurements are displayed in colored lines while a shaded region is bounded by LOESS smoothed daily minimum and maximum values with a LOESS smoothed daily mean values for each site displayed with dashed black lines.*

Discrete water quality parameters showed significant variation as a result of varying water sources (i.e. Sacramento River, Butte Creek or some combination of sources), and flow rates which influence water residence times in the various habitats (Figure 5). Generally, observed patterns included increased indicators of food web productivity and metabolic activity such as: diel dissolved oxygen range which is an indication of stream metabolism (Jeffres et al., 2020), chlorophyll-α, and dissolved organic carbon in off-channel habitats compared to the channel habitats. These patterns were present in wet year 2019 especially on the descending limb of the flood events, but were more pronounced under dry conditions where channel and off-channel habitats were disconnected for long periods of time without flushing flow events.

Specific conductivity (SPC) variation among sites provided as indicator of flooding conditions and influence of river water sources. SPC values of the river channels remained in the 72.1-141.1 $\mu s \cdot cm^{-1}$ range for the Feather River and in the 122.9-195.6 range for the Sacramento River near Colusa. Butte Creek SPC values were more variable due to upstream agricultural and wetland water uses creating recirculated flows to the channel resulting in a range of 96.3-197.9 in the wet year to 152.6-359.3 in the dry years. This pattern was apparent in the pairwise comparisons of SPC values between habitats in the different years which confirmed the dominant influence of the Sacramento River as a water source in the wet year (2019) with no differences detected between habitat types (Figure 5). Conversely, in the dry years (2020 and 2021), the river habitat was the only distinct type indicating the dominant influence of the Butte Creek water source in the Butte Sink and Sutter Bypass sites during dry years (Figure 5).

Chlorophyll-α, which is a proxy for phytoplankton abundance (Stomp et al., 2011), was significantly higher in off-channel habitats compared to the river habitat in the wet year. However, in the dry years chl-α was not significantly different from channel habitats. Dissolved organic carbon exhibited the lowest values in river habitats and under high flow conditions. Interestingly, DOC levels

were relatively consistent across Sutter Bypass habitats including off-channel and canal channel habitats.

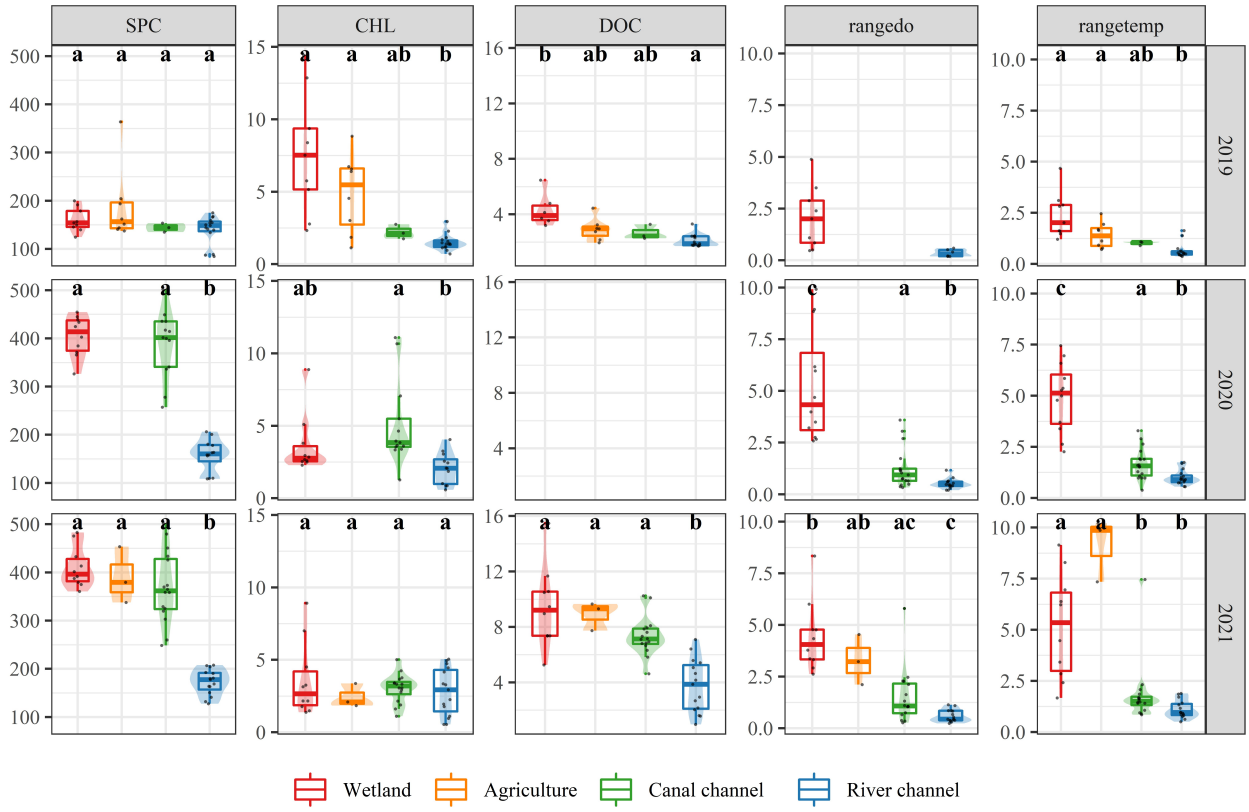

Figure 5. *Boxplots of water quality parameters corresponding to specific conductivity (SPC; µS⋆cm^{-1}), chlorophyll-α concentration (CHL; µg⋆L^{-1}), dissolved organic carbon (DOC; ppm), diurnal dissolved oxygen range (rangedo, mg⋆L^{-1}), and diurnal water temperature range (rangetemp; °C). Boxplots are grouped by habitat type (x-axis) and water year (vertical panels). Compact letter displays above the boxplots indicate significantly differentiated groups.*

Zooplankton

In all years, off-channel habitats had orders of magnitude higher total zooplankton abundances than river channel habitats (Figure 6). The only exception to this occurred during the 2019 high flow period in early March where flushing flows diluted the off-channel habitat zooplankton communities of the Butte Sink and Sutter Bypass, making them temporarily homogenous with river channel zooplankton densities (Figure 6A). Subsequent zooplankton production in off-channel habitats during the receding

limb of the flood pulse resulted in divergence in the zooplankton densities from the less productive river channel habitats.

Zooplankton community composition showed distinct differences between the four habitat types in all years (ANOSIM, 2019: R = 0.16, p-value = 0.003, NMDS stress = 0.10; 2020: R = 0.64, p-value < 0.001, NMDS stress = 0.14; 2021: R = 0.44, p-value < 0.001, NMDS stress = 0.12; supplemental figure A1). Despite distinct zooplankton assemblages between habitats in all years, differences were more pronounced in drier water years (2020 and 2021) as evidenced by higher ANOSIM R statistic values. Visual assessment of the global NMDS analysis supported this result and showed higher overlap in the wet year (2019) compared to the two dry years (NMDS stress = 0.14; Figure 6B). This analysis showed that the variance along the NMDS-1 axis was explained by relative density of large Cladocera to the left and aquatic to the right (Figure 6B). High productivity in off-channel habitats especially in the two dry years resulted in high densities of zooplankton including small- and large-bodied cladocerans, and copepods. River channel habitats tended to have proportionately higher densities of insects, particularly *Chironomidae sp.* midges. Wetlands supported extremely high concentrations of large Cladocera, particularly *Daphnia pulex*, and copepods dominated by *Acanthocyclops sp*. Canal channel habitats exhibited zooplankton assemblages dominated by small cladoceran species such as *Bosmina spp*. and C*eriodaphnia spp.* with a notably low abundance of large-bodied cladoceran spp. (e.g. *Daphnia pulex)* in the dry years 2020 and 2021 (Figure 6c). This observation was supported by the pairwise mean tests where in the two dry years, large bodied cladoceran densities were higher in the wetlands whereas small cladoceran densities were not different between canal channels and wetlands (Figure 6C).

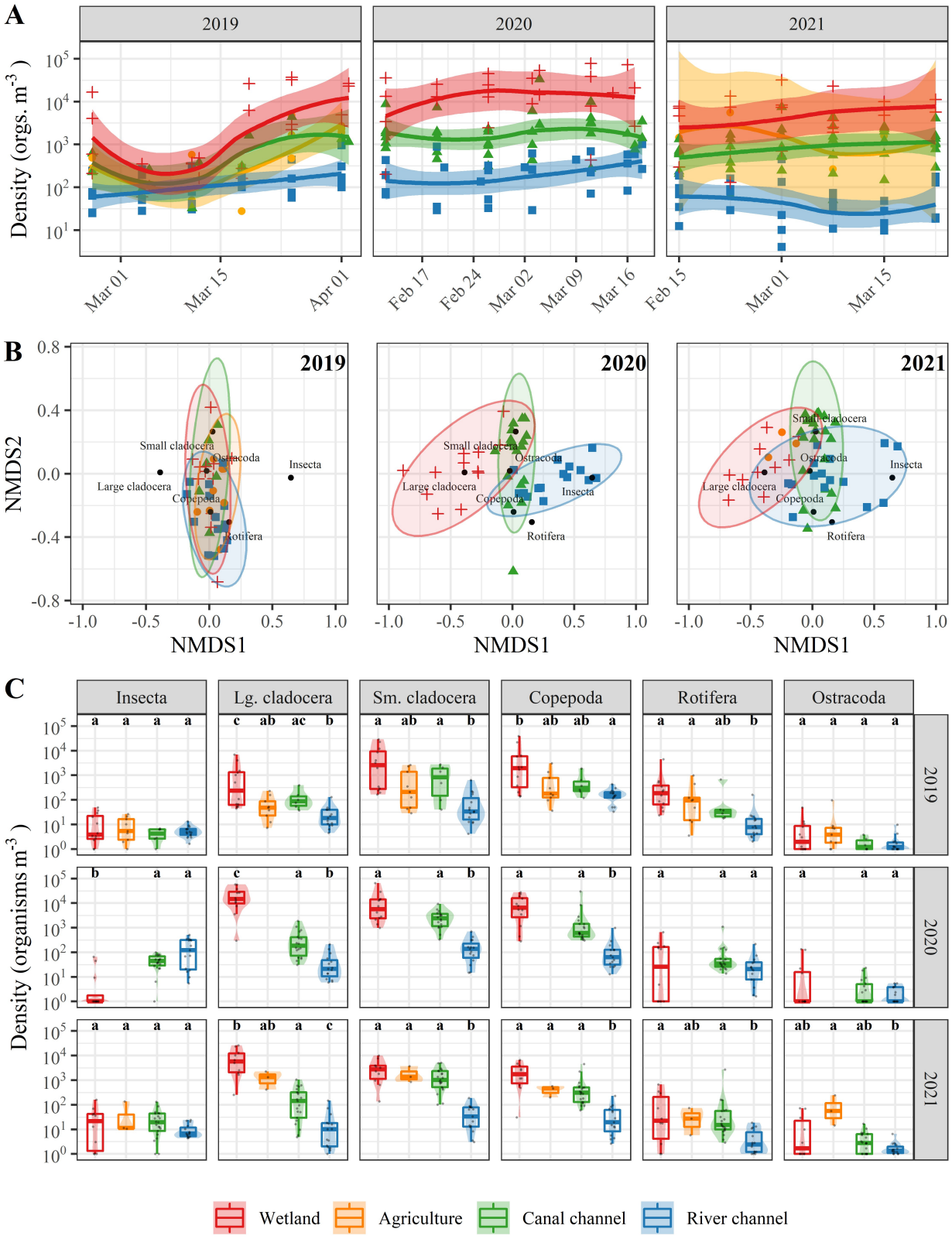
A
2019
2020
2021
Density (orgs. m-3)
Mar 01
Mar 15
Apr 01
Feb 17
Feb 24
Mar 02
Mar 09
Mar 16
Feb 15
Mar 01
Mar 15
B
2019
2020
2021
NMDS2
NMDS1
Small cladocera
Large cladocera
Ostracoda
Copepoda
Insecta
Rotifera
C
Insecta
Lg. cladocera
Sm. cladocera
Copepoda
Rotifera
Ostracoda
Density (organisms m-3)
Wetland
Agriculture
Canal channel
River channel

***Figure 6**. **Panel A**: Time series of total zooplankton density (organisms•m^{-3}) with loess smooth lines for each habitat type. **Panel B**: Results from the global NMDS analysis including data from all three years of the project with each year highlighted individually. **Panel C**: Boxplots grouped by habitat type and separated by HTU (top bar) and year (side bar). Note the log_{10} scaled on the y-axes of panels A and C.*

Enclosure salmon diets

Similar to the zooplankton community analysis (above) enclosure reared salmon diet contents showed distinct patterns between habitats, but these patterns were much more pronounced in 2020 and 2021 (dry years) versus 2019 (ANOSIM, 2019: R = 0.20, p-value = 0.10, NMDS stress = 0.04; 2020: R = 0.58, p-value < 0.001, NMDS stress = 0.05; 2021: R = 0.42, p-value = 0.003, NMDS stress = 0.03, supplemental figure A2). Enclosure-reared salmon at river sites tended to have diets dominated by insect taxa (primarily Chironomidae) in all years (Figure 7A). The SRC4 site downstream of the Sutter Bypass and Sacramento River confluence exhibited greater variance and grouped closer to Sutter Bypass sites in the wet year (2019). Enclosure-reared salmon in off-channel habitats tended to have diets composed predominantly of zooplankton species including cladocerans and copepods. Wetland fish also showed a consistently higher abundance of amphipods in their diets in all years. Insects played a larger role in the diets of off-channel habitats in the wet year compared to the dry years. Salmon at canal channel sites did not exhibit a clear pattern in their diets with some closely resembling off-channel habitat diets while others more closely resembled river channel diets. The prey mass index (PMI) also did not have a clear signal between habitats (Figure 7C).

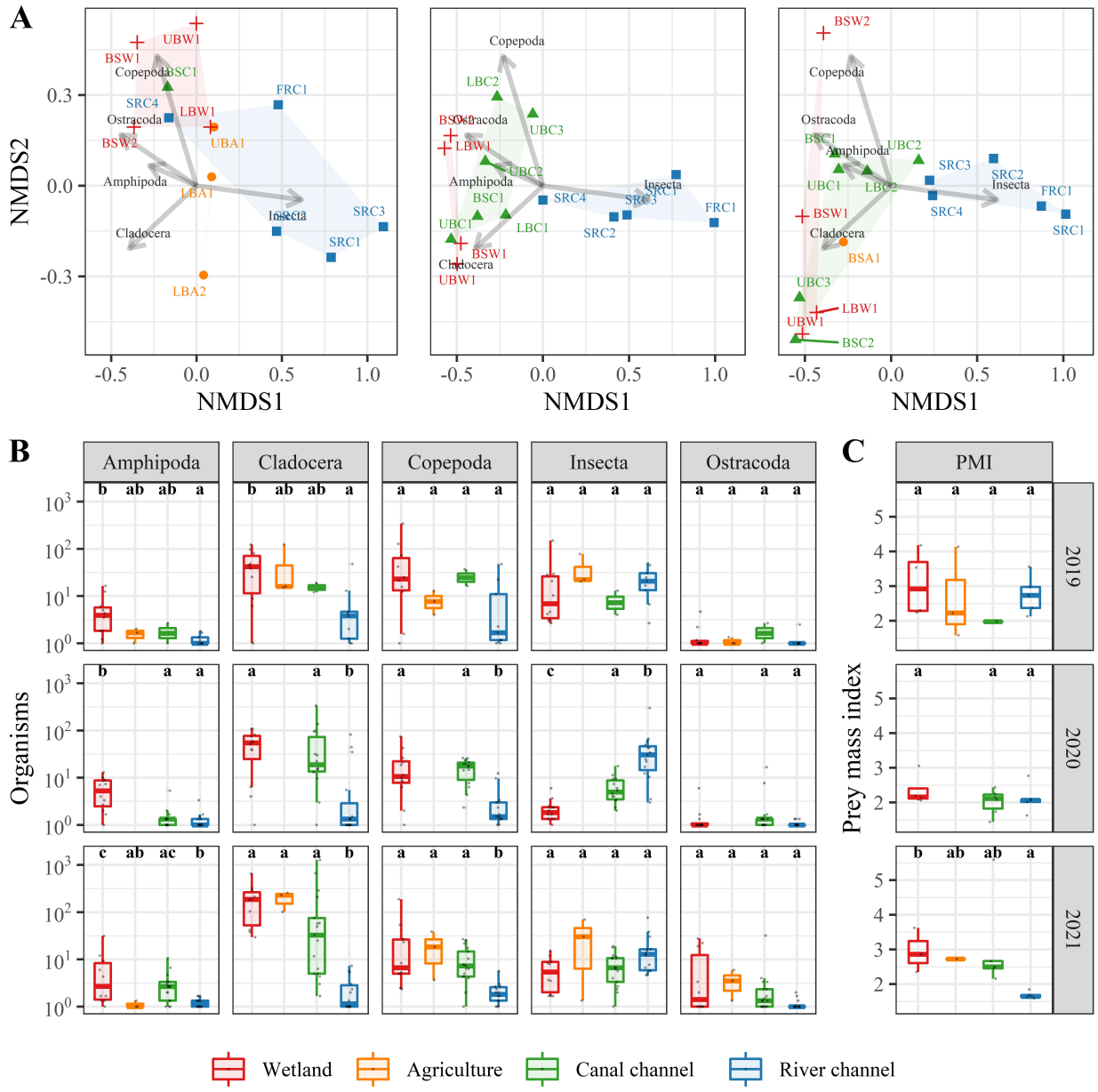

Figure 7. ***Panel A****: Results from a global NMDS analysis of diet assemblages by enclosure site including data from all three years of the project with each year highlighted individually.* ***Panel B****: Boxplots of mean prey items for each site grouped by habitat type and separated by HTU (top bar) and year (side bar).* ***Panel C****: Boxplots of mean prey mass index (PMI) grouped by habitat type and year.*

Enclosure salmon growth

Mean individual mass growth rates of salmon across all year were significantly different between habitats (ANOVA, F-value = 9.405, p-value < 0.001, Table 3 and Figure 8B). Results from the

post-hoc Tukey pairwise comparisons revealed that wetland habitat growth rate was higher than river and canal channel habitats, but not distinguishable from agriculture habitat (Figure 8C).

***Table 3**. Summary table of mean enclosure-reared salmon fork length (FL) and mass growth rates by habitat type. N = number of enclosure sites.*

Habitat type	Mean FL growth rate ($mm \cdot day^{-1}$)	Mean mass growth rate ($g \cdot day^{-1}$)	FL growth rate range ($mm \cdot day^{-1}$)	Mass growth rate range ($g \cdot day^{-1}$)	N
Wetland	0.63 ± 0.20	0.10 ± 0.05	0.36 - 0.98	0.05 - 0.21	12
Agriculture	0.48 ± 0.15	0.07 ± 0.03	0.31 - 0.68	0.04 - 0.12	4
Canal channel	0.28 ± 0.24	0.04 ± 0.05	0.08 - 0.89	0.00 - 0.19	12
River channel	0.24 ± 0.07	0.03 ± 0.01	0.15 - 0.37	0.01 - 0.04	15

Enclosure-reared Chinook Salmon reared in wetland habitats exhibited the highest growth rates in all years and the highest rates during periods of low river connectivity and higher residence time conditions during dry water years (2020 and 2021). These growth rates were comparable to those observed in free-ranging juvenile salmon reared in off-season rice fields in the Yolo Bypass which were among the highest recorded growth rates of juvenile Chinook Salmon in the Central Valley (Holmes et al., 2021). Juvenile salmon in agriculture sites in the Bypass that experienced sustained flushing flows in 2019 had growth rates similar to adjacent river habitats. Fish from the lone agriculture site in 2021 showed much higher growth rates (0.68 $mm \cdot day^{-1}$) which were similar to average wetland growth rates. Canal channel sites displayed the greatest heterogeneity (range 0.08-0.89 $mm \cdot day^{-1}$) in growth rate, containing both the lowest growth rate (at BSC1 in year 2020) and the second highest growth rate (at BSC2 in 2021). This variability in salmon growth rates at canal channel sites exhibited a longitudinal trend where the fastest growth rates were observed immediately downstream of the Butte Sink wetlands and diminished in the Sutter Bypass. River channel sites showed stable, moderate growth with the least heterogeneity (range 0.15-0.37 $mm \cdot day^{-1}$) within and between years compared to the other habitat types.

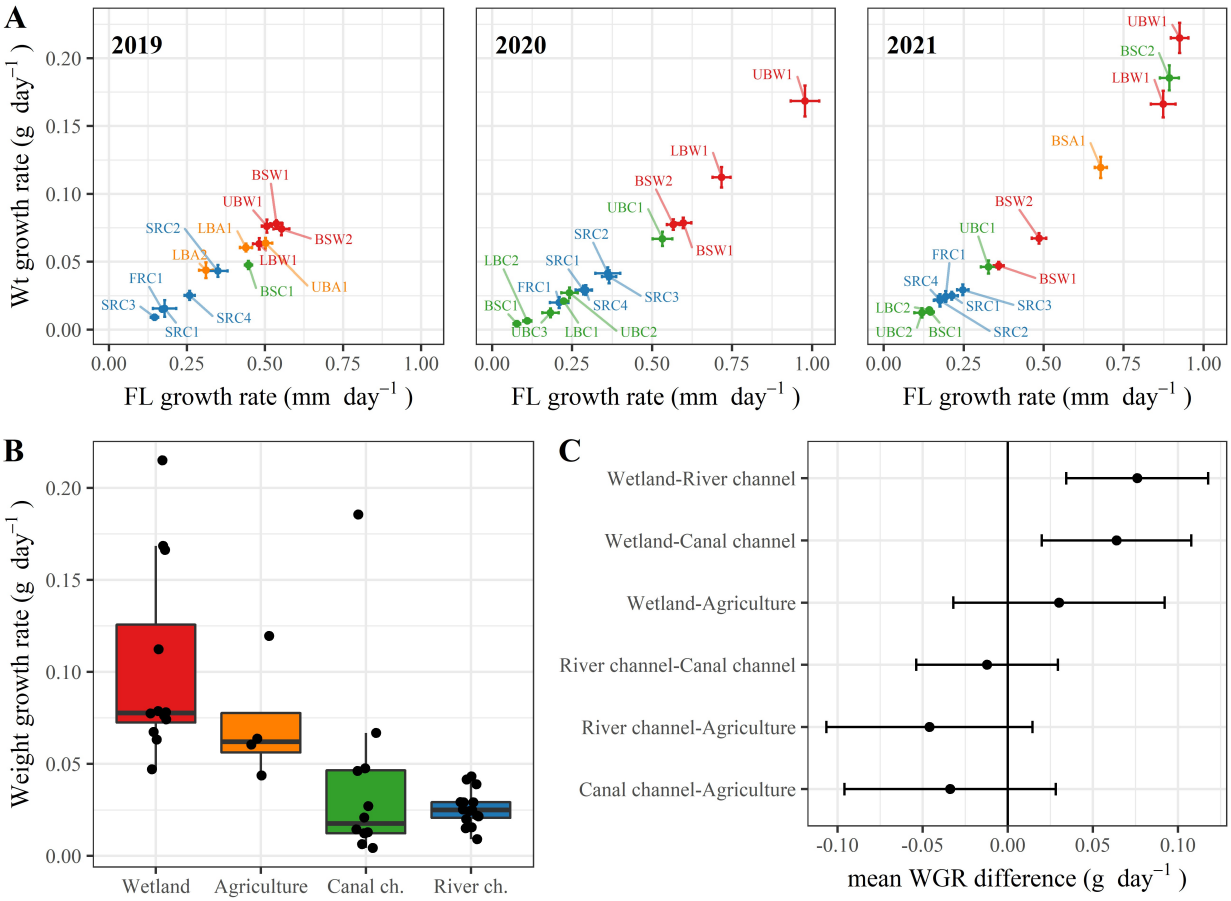

Figure 8. ***Panel A****: Biplots showing means (points) and standard errors (lines) of fork length (x-axis) and weight (y-axis) growth rates for each enclosure location colored by habitat type.* ***Panel B****: Boxplots of mean growth rates by habitat type.* ***Panel C****: Pairwise comparison of mean weight growth rate between habitat types where the points represent the difference between the means. Pairwise comparisons in which the 95% confidence intervals do not overlap with zero are statistically significant.*

Mass specific growth rate correlates

Food web explanatory variables were the most informative for predicting observed salmon growth rate response (Figure 8). Log transformed large cladoceran density was the most important predictor of salmon growth. This result was consistent with findings from Holmes et al. (2021) which showed that large-bodied Cladocera species (e.g. *Daphnia pulex*) accounted for over 90% of the juvenile salmon gut contents in off-channel rice fields. Visual analysis of the partial dependence plots (Figure 8) appeared to identify a potentially important threshold effect indicating high growth potential above a $\log_{10}$ transformed large Cladocera density of approximately 3 which is equal to 1,000 organisms$\cdot$m^{-3}.

There was also a positive association between chlorophyll-α and salmon growth response which is consistent with findings from Corline et al. (2021) which showed that chlorophyll-α was a strong predictor of zooplankton abundance. Salmon growth rate response was also positively associated with increased Rotifer abundance. Conversely, salmon growth response to insect densities created an unexpected result where an inverse relationship between ambient insect densities and salmon growth rate response was observed (Figure 8). Mean daily water temperature range was the abiotic factor which most strongly predicted growth rates and had a positive relationship. Turbidity was the second most informative abiotic factor. Mean temperature was a weak predictor of salmon growth rate in this experiment which was an unexpected result due its importance in bioenergetics modeling (Warren and Davis, 1967).

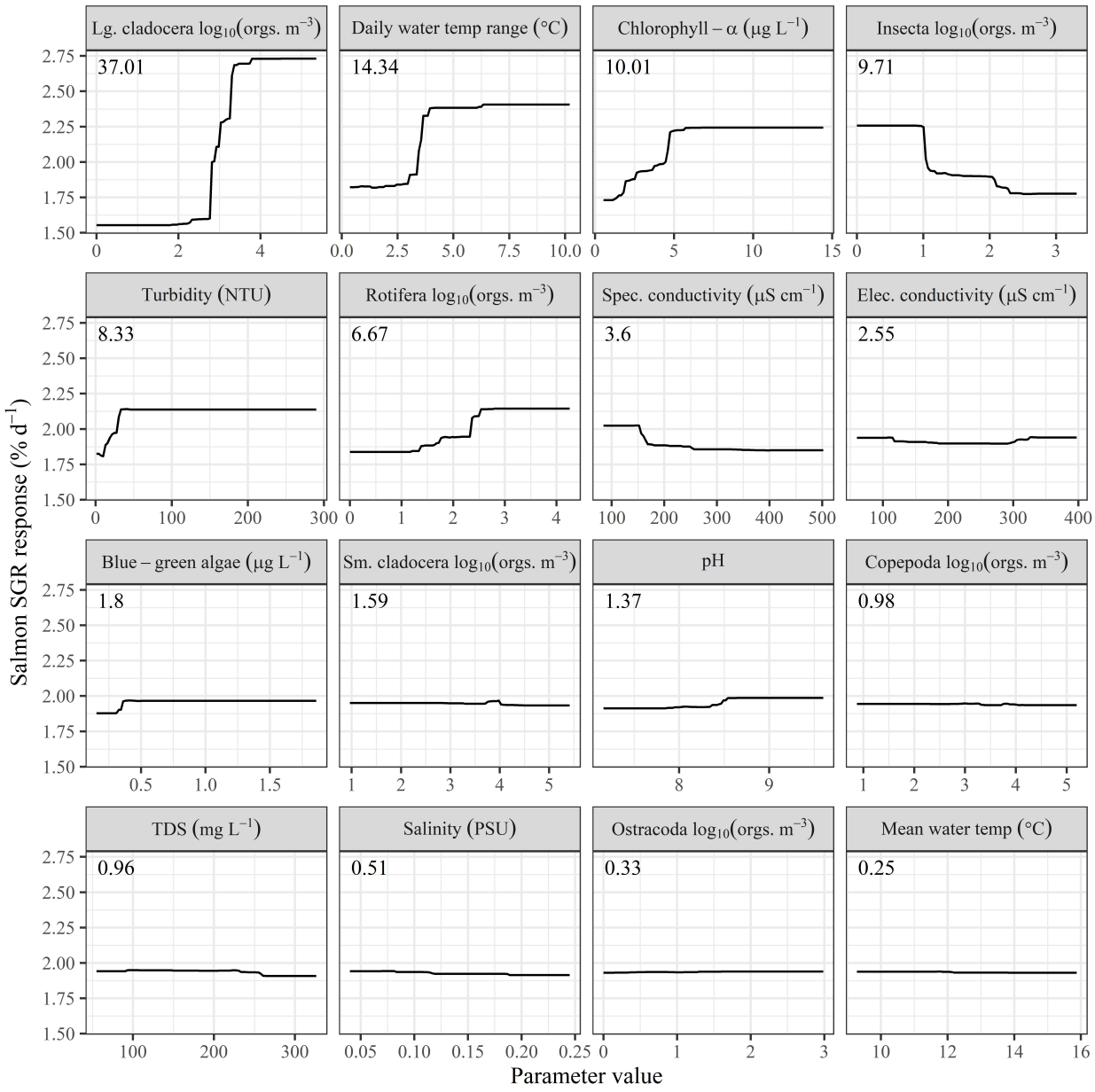

Figure 8*. Partial dependence plots from the BRT analysis showing functional response of mass specific growth rate (y-axis) over the range of the explanatory variable parameter values (x-axis). Relative importance value for each predictor variable is printed in the top left corner of each plot.*

Wild salmon occupancy

Results from the concurrent wild fish sampling showed that juveniles of all four Chinook Salmon runs found in the CCV (winter-run, spring-run, fall-run, and late fall-run) were observed in the Sutter Bypass (Table 4; Figure 9A). In 2019, juvenile Chinook Salmon (n = 147) were sampled in the Sutter

Bypass, of which 44 were caught immediately downstream of the Colusa and Tisdale weirs during overtopping events, 3 were caught in the bypass while it was flooding along the margins, and 100 were caught in off-channel habitats (wetlands and agricultural fields) while floodwaters drained. Winter-run (n = 22) were only observed in 2019 and were more prevalent early in the season (Figure 9A). In 2020, a small early-season flow pulse from Butte Creek in late January 2020 brought juvenile spring-run Chinook Salmon fry into the Butte Sink wetland where we had an enclosure site, BSW1. The mean size of a sample of the entrained wild origin fry was 40mm ± 2.2mm SD and 0.51g ± 0.11g SD on February 4th, 2020. Repeated sampling of this relatively closed population yielded an apparent growth rate of approximately 0.65 mm·day^{-1} which was consistent with the enclosure-reared salmon concurrently in the same wetland which had a mean growth rate of 0.60 mm·day^{-1} (Figure 9B).

Table 4*. All wild juvenile Chinook Salmon caught by year and genetic run type. Numbers in parenthesis represent the number of fish with clipped adipose fins.*

	Fall	**Late fall**	**Spring**	**Winter**	**Undetermined**	**Total**
2019	36 (7)	5	82	22	2	147 (7)
2020	1		59		8	68 (0)
2021	37 (1)	6	88		29	160 (1)
Total	74	11	229	22	39	375 (8)

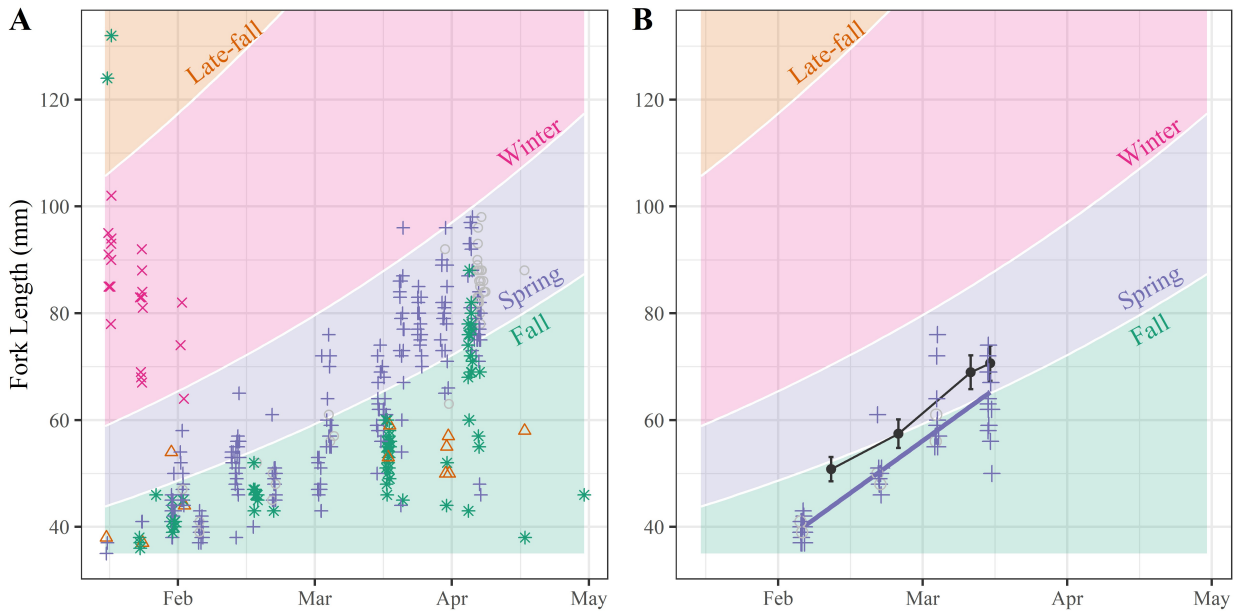

Figure 9. *Scatter plots of salmon fork length on the y-axis and date of capture on the x-axis. Delta model size at date run classifications are provided as a background for context of relative performance compared to population level average growth trajectories.* ***Panel A:*** *Wild juvenile Chinook Salmon caught during the experiment with color and shape of points corresponding to genetic run assignment (Pink (x) = winter-run, purple (+) = spring-run, green (*) = fall-run, orange (△) = late fall-run.* ***Panel B:*** *Scatterplot of size at date for a group of wild spring run juveniles (purple crosses) which were entrained in a Butte Sink wetland in late January 2020 until drainage in March 2020. Black points and lines correspond to BSW1 mean enclosure growth concurrently in the same wetland.*

Wild salmon diets

Diets from wild-caught juvenile Chinook Salmon were similar to that of enclosure reared salmon. River-caught salmon from the Sacramento River and immediately downstream of the weirs had diets composed primarily of aquatic insects (Figure 10A). Salmon caught in and near off-channel habitats in the Butte Sink had diets composed primarily of cladocerans and copepods (Figure 10A). Salmon caught in the canals and agricultural fields of the Sutter Bypass displayed greater variability with a mix of insect and zooplankton based diets. Visual inspection of a global NMDS analysis (Stress = 0.07) including data from all three years supported these general results with Butte Sink locations to the left, Sacramento River locations to the right, and Sutter Bypass locations which spanned the full range (Figure 10B).

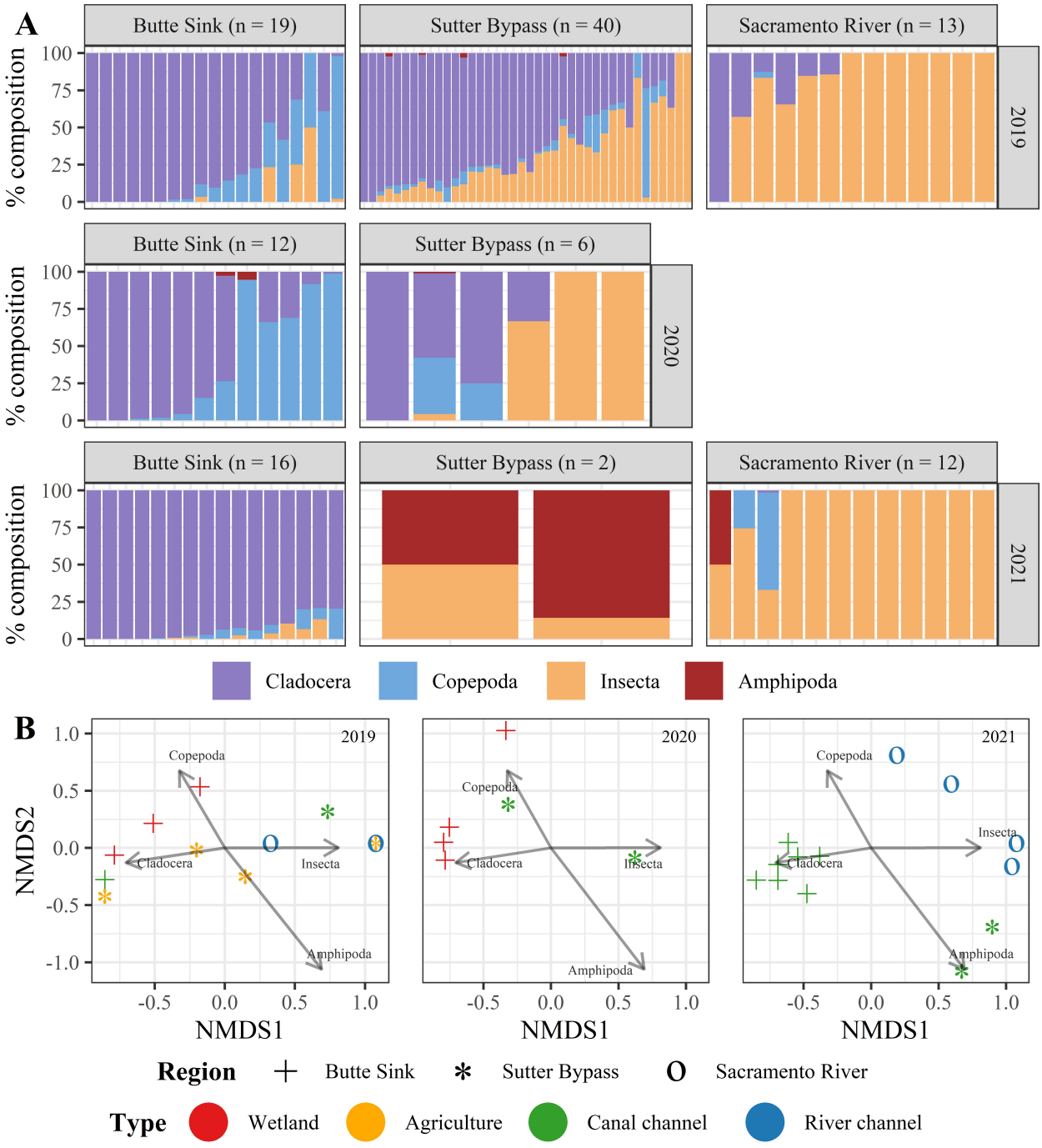

Figure 10: Panel A: *Bar plots showing percent abundance of stomach contents from each analyzed wild juvenile Chinook Salmon grouped by region and year.* ***Panel B:*** *NMDS analysis of mean gut composition for each sampling site/week/year combination symbolized by region (shapes) and habitat type (color).*

Discussion:

Despite broad consensus on the need to improve habitat quality for juvenile Chinook Salmon (Herbold et al., 2018), uncertainty in the expected biological response to alterations of the abiotic and biotic environment inhibits effective restoration and management efforts. Implementation of an enclosure experiment, which measured the growth rate response of juvenile Chinook Salmon in association with ambient water quality and lower trophic metrics, permitted the assessment of habitat quality across the CCV landscape under hydrologic extremes. Understanding the resulting variance in growth rate response has implications for population level effects since early ocean survival of Chinook Salmon correlates positively with size at ocean entry (Woodson et al., 2013). Salmon growth enclosure experiments confirmed results from previous studies which demonstrated improved growing conditions in floodplain habitats associated with increased food production and prey availability (Sommer et al., 2001a; Jeffres et al., 2008; Katz et al., 2017; Cordoleani et al., 2022). Yet, some surprising patterns emerged between water year types and across habitat components. Findings suggest that growth potential of juvenile salmon is 1) variable through time and dependent on hydrologic conditions and 2) variable through space and strongly dependent on prey availability in various habitat types. The observed homogenization of the food web, thermal profiles, and salmon growth potential under high flow conditions was not necessarily surprising provided previously identified effects of hydrology on food web processes (Ahearn et al., 2006; Grosholz and Gallo, 2007). However, such effects have not been documented with this degree of trophic level specification and spatiotemporal coverage previously. In human-dominated landscapes like the CCV, these results highlight the complexity of management aimed at restoring sufficient quantity and quality of habitats needed for ecosystem function while meeting critical societal needs of flood protection and agriculture.

Severe droughts experienced in the past decade bring the socioecological importance of CCV floodplains into even higher relief. The response of salmon to the two drought years observed in this study are valuable for understanding how the CCV habitat mosaic functions for juvenile Chinook Salmon

under drought conditions. During periods of low connectivity between channel and off-channel habitats, distinct signatures of water quality conditions and food web processes are detectable between habitats. The key indicators include physical metrics of higher conductivity and higher diurnal variation in temperature and dissolved oxygen and correlate with higher basal food-web productivity and zooplankton abundances in off-channel habitats. The highest salmon growth rates observed in this study were under drought conditions that involved low connectivity. Here, the floodplain food web was able to more fully develop and be maintained by existing wetland or agricultural infrastructure (e.g. berms, swales, water control structures). Ultimately, wild salmon access and food web development create an apparent conundrum where the highest growth rates in this region are unavailable to migrating fish in the main-stem rivers under current water operations. However, conservation actions are being developed which can increase direct access to off-channel habitats for migrating fish via functional flow pulses (Yarnell et al., 2015; Yarnell et al., 2020) and infrastructure modifications which enhance fish passage (e.g. weir notches) and extend flood water inundation time (Sommer et al., 2020). Such measures can enhance fish benefit with efficient water allocation.

In addition to direct benefits to juvenile Chinook Salmon which access off-channel habitats, indirect effects of off-channel habitats on downstream channel food webs and fish response were observed in this experiment. These effects were widespread in 2019 where inundation of large areas of the Butte Sink and Sutter Bypass led to a diverse zooplankton community and elevated salmon growth potential at key points downstream of return flow points from the Butte Sink near Colusa and downstream of the Sacramento River and Sutter Bypass Confluence. Both areas showed high relative salmon growth and the presence of key off-channel zooplankton indicator species (Corline et al., 2021). Surprisingly, we observed a general underperformance of salmon in canal channel habitats in the Sutter Bypass given the benign water quality parameters and elevated ambient zooplankton densities. Despite overall underperformance, close proximity downstream of a substantial wetland effluent point which

provided a source of high invertebrate production and passive dispersal, resulted in salmon growth potential at two canal sites which was comparable to wetland habitats. The observed longitudinal depletion of larger prey items as a function of distance from wetland effluent points may indicate the need for more interspersed off-channel subsidies with regular spacing on the landscape, akin to a "string of pearls" restoration objective (Gustafson and Parker, 1994). The competitive grazing hypothesis is consistent with the observation from Brooks and Dodson (1965) where large zooplankton species were depleted in the presence of a zooplanktivorous predator, alewife (*Alosa psuedoharangus*). Another explanation for the observed growth rate reduction is the potential that these channels receive harmful pollutants and pesticides in effluent from municipal and agricultural runoff which limits autochthonous production of sensitive invertebrate prey taxa (Palmer et al., 2010; Anzalone et al., 2022). While we cannot rule out this hypothesis, there is little-to-no data on the history and persistence of agricultural pollution in these habitats. A more plausible current explanation is the trophic influence of high densities of resident zooplanktivorous fishes (Table A1; also see Feyrer et al., 2006) which selectively graze down the large allochthonous prey resources. Restoration of these degraded channel habitats may require a multifaceted effort involving reconnection of off-channel habitats along with management of invasive species to achieve the desired ecological response.

The BRT analysis showed that the factors most strongly correlated with increased juvenile salmon growth tended to be food web factors including density of zooplankton prey and chlorophyll-α production. The key finding from that analysis indicated a potentially important density threshold of approximately 1,000 large cladoceran individuals$\cdot m^{-3}$ needed for maximal Chinook Salmon growth potential. Interestingly, physical factors (e.g. mean water temperature, conductivity, turbidity, and pH) did not correlate with salmon growth to the extent of food web factors in our experiment. This may be a result of those factors having lagged effects on the food web which decreases the direct linkage between the physical hydrologic and water quality conditions and salmon growth response. One

example of this complex response was specific conductivity patterns which have previously been identified as a strong predictor of residence time and food web development (Corline et al., 2021). In our study, specific conductivity described very little variance in salmon growth, which is likely a result of variable water sources with different conductivity baselines as well as top down grazing pressures which can deplete zooplankton rich water of high value prey items especially in perennial waterways. The physical factor most strongly linked to salmon growth rate response was diurnal temperature range. While this was a key finding, previous research has shown that it is unlikely that this linkage has a direct effect on salmon growth (Imholt et al., 2011). It is more likely that the conditions driving high diel temperature variation (e.g. shallow depth, low connectivity, high residence time) are also tightly correlated with conditions conducive for high zooplankton production. Similarly, the fact that off-channel habitats had lower dissolved oxygen levels than channel habitats showed how increased ecosystem metabolic activity was correlated with high prey abundance rather than a direct effect on salmon development (Aha et al., 2021). At several points in the experiment, dissolved oxygen measurements below 1.5 $mg{\cdot}L^{-1}$ occurred for prolonged periods. These values are well below previous levels (< $3mg{\cdot}L^{-1}$) believed to be a threshold for increased lethality for juvenile salmonids (Chapman, 1986), or which may induce avoidance behavior (Carter, 2005). However, enclosure-reared salmon in our study sites which encountered hypoxic conditions maintained fast growth rates. We cannot rule out the potential for indirect survival effects on wild salmon due to reduced swimming performance in hypoxic conditions (Davis et al. 1963). Furthermore, it is unclear if enclosure effects in our study permitted lethargy or other behavioral adaptations (e.g. vertical movement in the water column), which may increase susceptibility to predation in the wild, to survive the hypoxic conditions. Further research into physiological and behavioral coping mechanisms of juvenile salmon in habitats with hypoxic conditions is needed.

Our concurrent sampling of wild fish in the Sutter and Bypass and adjacent habitats yielded insights which are compatible with the findings from the enclosure experiment and lower trophic sampling. Specifically, our observation that the wild fish assemblages were dominated by juvenile salmon (Table A1) from all four runs in the winter and early spring months can guide potential future water management decisions. Wild-caught juvenile salmon in and near off-channel habitats in the Butte Sink and Sutter Bypass were shown to have diets dominated by zooplankton prey taxa consistent with enclosure-reared salmon in the vicinity. The enhanced growth conditions for salmon accessing off-channel habitats indicated by our enclosure experiment are likely to be realized by juvenile salmon early in the migratory season (i.e. December to March) with more benign water temperatures in the off-channel habitats than would be expected later in the migratory period (Kjelson and Raquel, 1982). Early season off-channel habitat access could increase the abundance of ocean-ready juveniles earlier in the season before downstream water quality conditions and predator activity in the California Delta have reached detrimental levels (Nobriga et al., 2021). Indeed, our observation of large Butte Creek salmon early in the season may explain the improved performance of this population compared to other spring-run Chinook Salmon populations which have remained low in recent years (Cordoleani et al., 2020). This underscores the importance of providing access to off-channel habitats for other Central Valley juvenile Chinook Salmon populations early in the migration season to enhance the portfolio of rearing and migration strategies.

Understanding the value of certain habitats and how the opportunities provided to juvenile salmon is of paramount importance to improved management of water resources and infrastructure modifications. Direct access to off-channel habitats and indirect benefits of food subsidies in channel habitats generate variable growth conditions for populations of juvenile salmon across the landscape. Enhancing these opportunities will promote a more heterogeneous mix of life-history strategies which may boost population resiliency (Carlson and Satterthwaite, 2011). Results from these experiments

demonstrate that the process of inundating off-channel habitats whether by large-scale weir overtopping or managed flooding creates distinct water conditions correlated with increased invertebrate prey densities, improved foraging conditions, and ultimately higher somatic growth rates for juvenile Chinook Salmon. This supports the concept that multi-function flood bypasses can play an important role in altered riverscapes by providing ecosystem services for society and improving rearing conditions for juvenile Chinook Salmon.

References:

Aarts, B. G. W., F. W. B. Van Den Brink, and P. H. Nienhuis. 2004. Habitat loss as the main cause of the slow recovery of fish faunas of regulated large rivers in Europe: the transversal floodplain gradient. River Research and Applications 20(1):3–23.

Aha, N. M., P. B. Moyle, N. A. Fangue, A. L. Rypel, and J. R. Durand. 2021. Managed wetlands can benefit juvenile Chinook Salmon in a tidal marsh. Estuaries and Coasts 44(5):1440–1453. Springer.

Ahearn, D. S., J. H. Viers, J. F. Mount, and R. A. Dahlgren. 2006. Priming the productivity pump: flood pulse driven trends in suspended algal biomass distribution across a restored floodplain. Freshwater Biology 51(8):1417–1433. Wiley Online Library.

Anzalone, S. E., N. W. Fuller, K. E. H. Hartz, C. A. Fulton, G. W. Whitledge, J. T. Magnuson, D. Schlenk, S. Acuña, and M. J. Lydy. 2022. Pesticide residues in juvenile Chinook salmon and prey items of the Sacramento River watershed, California–A comparison of riverine and floodplain habitats. Environmental Pollution 303:119102. Elsevier.

Arthington, A. H., and S. R. Balcombe. 2011. Extreme flow variability and the boom and bust ecology of fish in arid-zone floodplain rivers: a case history with implications for environmental flows, conservation and management. Ecohydrology 4(5):708–720.

Benedict, M. A., and E. T. McMahon. 2012. Green infrastructure: linking landscapes and communities. Island press

Brooks, J. L., and S. I. Dodson. 1965. Predation, body size, and composition of plankton. Science 150(3692):28–35. NY.

Carlson, S. M., and W. H. Satterthwaite. 2011. Weakened portfolio effect in a collapsed salmon population complex. Canadian Journal of Fisheries and Aquatic Sciences 68(9):1579–1589. NRC Research Press.

Carter, K. 2005. The effects of dissolved oxygen on steelhead trout, coho salmon, and chinook salmon biology and function by life stage. California Regional Water Quality Control Board, North Coast Region 10.

Chapman, G. 1986. Ambient water quality criteria for dissolved oxygen. US Environmental Protection Agency, Office of Water Regulations and Standards. EPA 440/5-86-003.

Cordoleani, F., W. H. Satterthwaite, M. E. Daniels, and M. R. Johnson. 2020. Using Life-Cycle Models to Identify Monitoring Gaps for Central Valley Spring-Run Chinook Salmon. San Francisco Estuary and Watershed Science 18(4).

Cordoleani, F., E. Holmes, M. Bell-Tilcock, R. C. Johnson, and C. Jeffres. 2022. Variability in foodscapes and fish growth across a habitat mosaic: Implications for management and ecosystem restoration. Ecological Indicators 136:108681. Elsevier.

Corline, N. J., R. A. Peek, J. Montgomery, J. V. E. Katz, and C. A. Jeffres. 2021. Understanding community assembly rules in managed floodplain food webs. Ecosphere 12(2):e03330. Wiley Online Library.

Davis, G. E., J. Foster, C. E. Warren, and P. Doudoroff. 1963. The influence of oxygen concentration on the swimming performance of juvenile Pacific salmon at various temperatures. Transactions of the American Fisheries Society 92(2):111–124. Wiley Online Library.

Dettinger, M. 2011. Climate change, atmospheric rivers, and floods in California–a multimodel analysis of storm frequency and magnitude changes 1. JAWRA Journal of the American Water Resources Association 47(3):514–523. Wiley Online Library.

Dumont, H. J., I. Van de Velde, and S. Dumont. 1975. The dry weight estimate of biomass in a selection of Cladocera, Copepoda and Rotifera from the plankton, periphyton and benthos of continental waters. Oecologia 19(1):75–97. Springer.

Elith, J., J. R. Leathwick, and T. Hastie. 2008. A working guide to boosted regression trees. Journal of animal ecology 77(4):802–813. Wiley Online Library.

Feyrer, F., T. Sommer, and W. Harrell. 2006. Importance of Flood Dynamics versus Intrinsic Physical Habitat in Structuring Fish Communities: Evidence from Two Adjacent Engineered Floodplains on the Sacramento River, California. North American Journal of Fisheries Management 26(2):408–417. Taylor & Francis.

Foley, J. A., R. DeFries, G. P. Asner, C. Barford, G. Bonan, S. R. Carpenter, F. S. Chapin, M. T. Coe, G. C. Daily, and H. K. Gibbs. 2005. Global consequences of land use. science 309(5734):570–574. American Association for the Advancement of Science.

Fretwell, J. D., J. S. Williams, and P. J. Redman. 1996. National water summary on wetland resourcesVol. 2425. US Government Printing Office.

Garone, P. 2020. The fall and rise of the wetlands of California's Great Central Valley. University of California Press.

Geist, J. 2011. Integrative freshwater ecology and biodiversity conservation. Ecological Indicators 11(6):1507–1516. Elsevier.

Grosholz, E., and E. Gallo. 2006. The influence of flood cycle and fish predation on invertebrate production on a restored California floodplain. Hydrobiologia 568(1):91–109. Springer.

Gustafson, E. J., and G. R. Parker. 1994. Using an index of habitat patch proximity for landscape design. Landscape and urban planning 29(2–3):117–130. Elsevier.

Hansen, M. J., D. Boisclair, S. B. Brandt, S. W. Hewett, J. F. Kitchell, M. C. Lucas, and J. J. Ney. 1993. Applications of bioenergetics models to fish ecology and management: where do we go from here? Transactions of the American Fisheries Society 122(5):1019–1030. Taylor & Francis.

Herbold, B., S. M. Carlson, R. Henery, R. C. Johnson, N. Mantua, M. McClure, P. B. Moyle, and T. Sommer. 2018. Managing for salmon resilience in California's variable and changing climate. San Francisco Estuary and Watershed Science 16(2).

Hijmans, R. J., S. Phillips, J. Leathwick, J. Elith, and M. R. J. Hijmans. 2017. Package 'dismo.' Circles 9(1):1–68.

Holmes, E. J., and C. A. Jeffres. 2021. Juvenile Chinook Salmon Weight Prediction Using Image-Based Morphometrics. North American Journal of Fisheries Management 41(2):446–454. Wiley Online Library.

Holmes, E. J., P. Saffarinia, A. L. Rypel, M. N. Bell-Tilcock, J. V. Katz, and C. A. Jeffres. 2021. Reconciling fish and farms: Methods for managing California rice fields as salmon habitat. PLoS ONE 16(2 February). Cold Spring Harbor Laboratory.

Imholt, C., I. A. Malcolm, P. J. Bacon, C. N. Gibbins, C. Soulsby, M. Miles, and R. J. Fryer. 2011. Does diurnal temperature variability affect growth in juvenile Atlantic salmon Salmo salar? Journal of Fish Biology 78(2):436–448. Wiley Online Library.

Jeffres, C. A., J. J. Opperman, and P. B. Moyle. 2008. Ephemeral floodplain habitats provide best growth conditions for juvenile Chinook salmon in a California river. Environmental Biology of Fishes 83(4):449–458. Springer.

Jeffres, C. A., E. J. Holmes, T. R. Sommer, and J. V. E. Katz. 2020. Detrital food web contributes to aquatic ecosystem productivity and rapid salmon growth in a managed floodplain. PloS one 15(9):e0216019. Public Library of Science San Francisco, CA USA.

Karanovic, I. 2012. Recent freshwater ostracods of the world: Crustacea, Ostracoda, Podocopida.

Katz, J., P. B. Moyle, R. M. Quiñones, J. Israel, and S. Purdy. 2013. Impending extinction of salmon, steelhead, and trout (Salmonidae) in California. Environmental Biology of Fishes 96(10):1169–1186. Springer.

Katz, J. V. E., C. Jeffres, J. L. Conrad, T. R. Sommer, J. Martinez, S. Brumbaugh, N. Corline, and P. B. Moyle. 2017. Floodplain farm fields provide novel rearing habitat for Chinook salmon. PLoS ONE 12(6):e0177409--16.

Knox, R. L., E. E. Wohl, and R. R. Morrison. 2022. Levees don't protect, they disconnect: A critical review of how artificial levees impact floodplain functions. Science of The Total Environment:155773. Elsevier.

Legendre, P., and E. D. Gallagher. 2001. Ecologically meaningful transformations for ordination of species data. Oecologia 129(2):271–280. Springer.

Merritt, R. W., and K. W. Cummins. 1996. An Introduction to the Aquatic Insects of North America, 4th edition. Kendall Hunt Publishing.

Nilsson, C., C. A. Reidy, M. Dynesius, and C. Revenga. 2005. Fragmentation and flow regulation of the world's large river systems. science 308(5720):405–408. American Association for the Advancement of Science.

Nobriga, M. L., C. J. Michel, R. C. Johnson, and J. D. Wikert. 2021. Coldwater fish in a warm water world: Implications for predation of salmon smolts during estuary transit. Ecology and Evolution 11(15):10381–10395. Wiley Online Library.

Oksanen, J., F. G. Blanchet, R. Kindt, P. Legendre, P. R. Minchin, R. B. O'hara, G. L. Simpson, P. Solymos, M. H. H. Stevens, and H. Wagner. 2013. Package 'vegan.' Community ecology package, version 2(9):1–295.

Opperman, J. J., G. E. Galloway, J. Fargione, J. F. Mount, B. D. Richter, and S. Secchi. 2009. Sustainable floodplains through large-scale reconnection to rivers. Science 326(5959):1487–1488. American Association for the Advancement of Science.

Palmer, M. A., H. L. Menninger, and E. Bernhardt. 2010. River restoration, habitat heterogeneity and biodiversity: a failure of theory or practice? Freshwater biology 55:205–222. Wiley Online Library.

R Core Team. 2022. R: A language and environment for statistical computing. R Foundation for Statistical Computing, Vienna, Austria. URL https://www.R-project.org/.

Rosenzweig, M. L. 2003. Win-win ecology: How the earth's species can survive in the midst of human enterprise. Oxford University Press, Oxford.

Schindler, S., F. H. O'Neill, M. Biró, C. Damm, V. Gasso, R. Kanka, T. van der Sluis, A. Krug, S. G. Lauwaars, and Z. Sebesvari. 2016. Multifunctional floodplain management and biodiversity effects: a knowledge synthesis for six European countries. Biodiversity and conservation 25(7):1349–1382. Springer.

Sommer, T. R., M. L. Nobriga, W. C. Harrell, W. Batham, and W. J. Kimmerer. 2001. Floodplain rearing of juvenile Chinook salmon: evidence of enhanced growth and survival. Canadian Journal of Fisheries and Aquatic Sciences 58(2):325–333. NRC Research Press.

Sommer, T., B. Harrell, M. Nobriga, R. Brown, P. Moyle, W. Kimmerer, and L. Schemel. 2001. California's Yolo Bypass: Evidence that flood control Can Be compatible with fisheries, wetlands, wildlife, and agriculture. Fisheries 26(8):6–16.

Sommer, T., B. Schreier, J. L. Conrad, L. Takata, B. Serup, R. Titus, C. Jeffres, E. Holmes, and J. Katz. 2020. Farm to Fish: Lessons from a Multi-Year Study on Agricultural Floodplain Habitat. San Francisco Estuary and Watershed Science 18(3).

Stomp, M., J. Huisman, G. G. Mittelbach, E. Litchman, and C. A. Klausmeier. 2011. Large-scale biodiversity patterns in freshwater phytoplankton. Ecology 92(11):2096–2107. Wiley Online Library.

Strayer, D. L., and D. Dudgeon. 2010. Freshwater biodiversity conservation: recent progress and future challenges. Journal of the North American Benthological Society 29(1):344–358.

Thorp, J. H., and A. P. Covich. 2009. Ecology and classification of North American freshwater invertebrates. Academic press.

Tockner, K., and J. A. Stanford. 2002. Riverine flood plains: present state and future trends. Environmental Conservation 29(3):308–330.Warren, C. E., and G. E. Davis. 1967. Laboratory studies on the feeding, bioenergetics, and growth of fish.

Wickham, H., W. Chang, and M. H. Wickham. 2016. Package 'ggplot2.' Create elegant data visualisations using the grammar of graphics. Version 2(1):1–189.

Woodson, L. E., B. K. Wells, P. K. Weber, R. B. MacFarlane, G. E. Whitman, and R. C. Johnson. 2013. Size, growth, and origin-dependent mortality of juvenile Chinook salmon Oncorhynchus tshawytscha during early ocean residence. Marine Ecology Progress Series 487:163–175.

Yarnell, S. M., G. E. Petts, J. C. Schmidt, A. A. Whipple, E. E. Beller, C. N. Dahm, P. Goodwin, and J. H. Viers. 2015. Functional flows in modified riverscapes: hydrographs, habitats and opportunities. BioScience 65(10):963–972. Oxford University Press.

Yarnell, S. M., E. D. Stein, J. A. Webb, T. Grantham, R. A. Lusardi, J. Zimmerman, R. A. Peek, B. A. Lane, J. Howard, and S. Sandoval-Solis. 2020. A functional flows approach to selecting ecologically relevant flow metrics for environmental flow applications. River Research and Applications 36(2):318–324. Wiley Online Library.

Yoshiyama, R. M., F. W. Fisher, and P. B. Moyle. 1998. Historical abundance and decline of chinook salmon in the Central Valley region of California. North American Journal of Fisheries Management 18(3):487–521. Taylor & Francis.

Supplemental information:

Zooplankton NMDS analyses separated by year

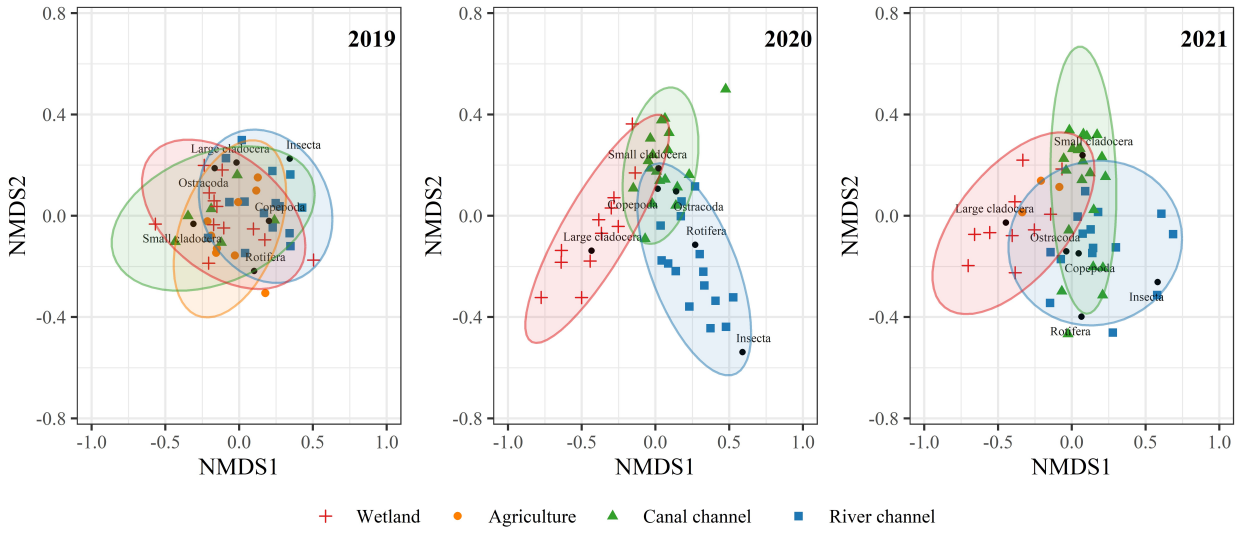

Figure A1. Plots of individual NMDS analyses for each year which correspond to the ANOSIM values presented in Zooplankton results section.

Enclosure salmon diet NMDS analyses separated by year

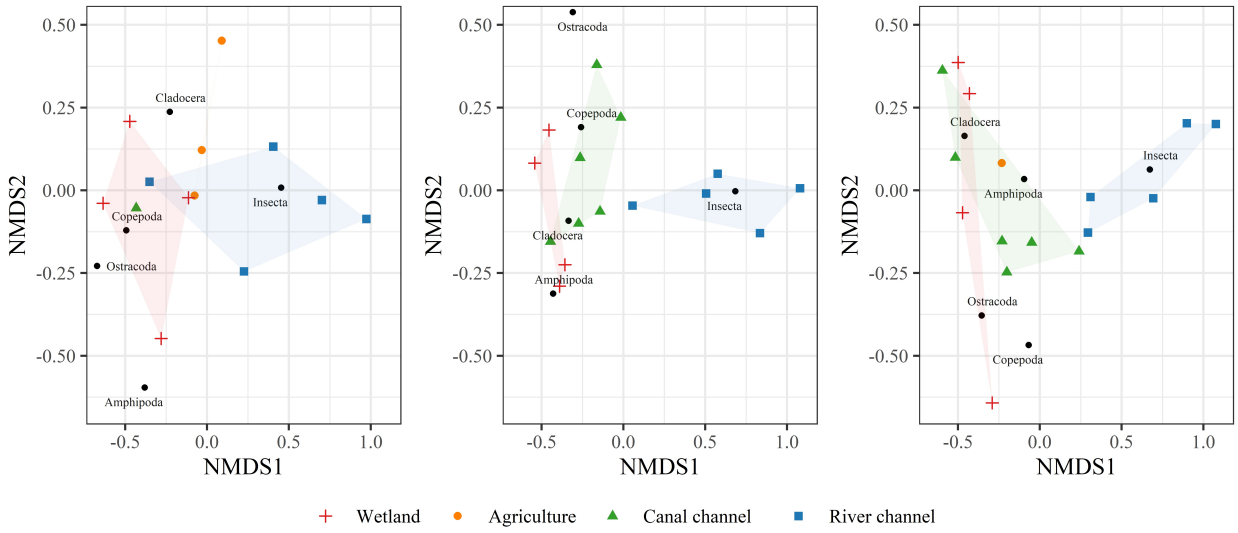

Figure A2. Plots of individual NMDS analyses for each year which correspond to the ANOSIM values presented in Enclosure salmon diets results section.

Fish assemblages

Overall, we observed 21 species of fish, of which 6 were native species (Table A1). In addition to Chinook Salmon, the most commonly encountered native fish species were Sacramento Pikeminnow (N = 63) and Sacramento Sucker (N = 13). We also noted the presence of steelhead (N = 6) in the Bypass in 2019, all of which appeared to be hatchery origin with clipped adipose fins. Mississippi silversides were the second most frequently encountered fish species. Silversides were observed only in the canal habitats and were rather patchily distributed with zero observed in 2020, but large numbers observed in 2021. This fish species tends to produce dense schools and one seine pull in a Sutter Bypass canal channel adjacent to the UBC1 enclosure site yielded 228 inland silversides. Bluegill were also caught with high frequency in our sampling efforts, many of which were young-of-the-year. Bluegills were encountered most frequently in the canal channels but were caught in river channels, agriculture, and wetland sites as well. Several non-native fish species were captured in this study which could potentially prey upon juvenile Chinook Salmon including adult sunfish species (e.g. Bluegill, Black Crappie, Largemouth Bass) and Brown Bullhead. These species assemblage results carry the caveat that the seining and fyke net sampling efforts were restricted to shallower areas and channel margins to due to gear limitations. Furthermore, sampling was directed to habitats and water bodies likely to contain juvenile Chinook Salmon and may over-represent their abundances compared to the other species.

***Table A1**. Summary of all fish species caught during the three-year experiment with total catch (N), mean, min and max fork length in millimeters. Asterisk next to species name denotes a native species.*

Species	Common name	N	Mean FL ± SD (mm)	min FL (mm)	max FL (mm)
*Oncorhynchus tshawytscha**	Chinook Salmon	393	63.9 ± 18.0	35	132
Menidia audens	Mississippi Silverside	295	80.1 ± 12.7	43	109
Lepomis macrochirus	Bluegill	102	82.0 ± 45.6	29	180
Notemigonus crysoleucas	Golden Shiner	98	76.1 ± 24.8	28	161
*Ptychocheilus grandis**	Sacramento Pikeminnow	63	71.6 ± 23.2	47	185
Lepomis gulosus	Warmouth	26	141.5 ± 22.2	102	185
Pomoxis nigromaculatus	Black Crappie	19	87.5 ± 24.3	55	146
Cyprinus carpio	Common Carp	16	174.2 ± 194.3	50	610
Lepomis cyanellus	Green Sunfish	15	109.7 ± 30.4	46	145
Percina macrolepida	Bigscale Logperch	14	90.4 ± 7.2	81	102
*Catostomus occidentalis**	Sacramento Sucker	13	78.7 ± 49.0	39	180
Gambusia affinis	Western Mosquitofish	11	32.5 ± 7.3	27	47
Micropterus salmoides	Largemouth Bass	9	118.3 ± 62.4	77	263
*Orthodon microlepidotus**	Sacramento Blackfish	7	27.1 ± 4.7	21	33
*Oncorhynchus mykiss**	Steelhead	6	204.7 ± 21.1	185	241
*Cottus asper**	Prickly Sculpin	5	69.2 ± 22.2	41	102
Dorosoma petenense	Threadfin Shad	4	98.3 ± 2.1	96	100
Pimephales promelas	Fathead Minnow	4	58.8 ± 9.3	45	65
Ameiurus nebulosus	Brown Bullhead	3	198.3 ± 56.2	150	260
Micropterus Sp.	Black Bass Sp.	2	65.5 ± 0.7	65	66
*Entosphenus tridentatus**	Pacific Lamprey	1	160	160	160
Lepomis microlophus	Redear Sunfish	1	129	129	129